U.S. DEPARTMENT OF COMMERCE
NATIONAL OCEANIC AND ATMOSPHERIC ADMINISTRATION
NATIONAL WEATHER SERVICE
NATIONAL METEOROLOGICAL CENTER

OFFICE NOTE 185

A Comparison of Two Global Analysis Systems in the Tropics

Glenn Rasch
Development Division

AUGUST 1978

A COMPARISON OF TWO GLOBAL ANALYSIS SYSTEMS IN THE TROPICS*

Glenn Rasch

National Meteorological Center, National Weather Service
Washington, D.C. 20233

ABSTRACT

An objective analysis system based upon the statistical optimum interpolation principle of Gandin has been developed at the National Meteorological Center, United States, for possible operational use during the period of the Global Weather Experiment. The performance of the analysis system in the Tropics is evaluated by comparison with the currently operational system, which employs a spectral objective analysis procedure. The operational system produces essentially nondivergent winds, an undesirable characteristic for an objective analysis system in the Tropics. In addition the operational system fails to make rational and systematic allowance for the varying error levels expected from the heterogeneous observing systems in the Tropics. The experimental system has been designed to overcome these shortcomings of the operational system. Evaluation in the Tropics is in part subjective: each system is judged according to the reasonableness of analyzed synoptic scale patterns. Objective evaluation includes calculation of statistical biases and statistical fit of analysis to observations. Finally, extended predictions to 72 hours, beginning from initial states prepared by each analysis method, are made and evaluated.

1. Introduction

An objective analysis system based upon the statistical optimum interpolation principle of Gandin (1963) has been developed at the National Meteorological Center (NMC), United States, for possible operational use during the First GARP Global Experiment (FGGE). One of the main characteristics of the FGGE data base will be its heterogeneous nature with respect to type and quality of observations. The FGGE data base will include observations from newly launched satellites such as TIROS-N, special aircraft reports including dropsondes, constant-level balloon observations, and observations from drifting buoys, in addition to the present operational data base. The analysis procedure has been specifically designed to account for the differing quality characteristics of the FGGE observing systems in a logical and systematic way.

---

*Paper presented at the RMS/RS/AMS Conference on Meteorology over Tropical Oceans, Aug. 21-25, 1978, at the Royal Meteorological Society's rooms in London, England.

An experimental version of the analysis method was recently tested in a 5½-day global data assimilation experiment. The purpose of this paper is to report on the results of that experiment in the tropical regions of the globe. The next section includes a description of the experimental assimilation system. Since the new system will be compared against the currently operational one, a brief description of the operational system is also included. Section 3 describes the test and methods used to judge the relative merits of the two systems. Results are presented in Section 4 followed by a summary. Throughout this paper the experimental system is referred to as the statistical method and the operational system as the spectral method.

2. Description of the Assimilation Systems

a. Statistical method

The two main elements of the statistical assimilation system are the optimum interpolation analysis (Bergman, 1976) and the NMC nine-layer global prediction model (Stackpole, et al., 1976). The prediction model serves as a vehicle for carrying forward in time the model representation of the atmosphere, providing a "guess" for each analysis.

Analysis

The analysis scheme is designed to update values of temperature and horizontal wind components at the grid points of the prediction model. It is multivariate: wind observations are used in the analysis of temperature and vice versa. Geostrophy, in the form of the thermal wind relationship, is used to determine the impact of one type of data on the other. Basically, the statistical method consists of minimizing the mean square analysis error. (See Bergman, 1976, for details on formulating the equations.) At each grid point, a set of linear equations can be solved for observational weights provided several statistical correlations and the observational errors are known. The correction applied to the guess at a grid point is then found by multiplying each weight by an observed correction and summing over all observations influencing the grid point.

Three kinds of correlation coefficients appear in the model equations. The first is the correlation of the guess error at one location with that at another location. This correlation is modeled by analytic functions and is based upon error statistics from the nine-layer model (Bergman and Gordon, 1977). The second is the correlation of the observational error at one location with that at another location. This correlation is assumed to be zero for most observing systems. Exceptions are satellite temperature errors, which are assumed to be correlated both horizontally and vertically, and rawinsonde temperature

and wind errors, which are assumed to be correlated in the vertical. These correlations are also modeled by analytic functions which are based upon various statistical studies. The third type of correlation coefficient is that between the guess error at one location and the observational error at another location. This correlation is assumed small in comparison to the other two and is therefore neglected.

Since the geostrophic balancing is not applicable at the equator, the temperature and wind analyses are gradually decoupled as the equator is approached. This is accomplished by multiplying the cross-correlations between temperature and wind components by an empirical function which decays to zero exponentially as the equator is approached and becomes unity at high latitudes.

The final quantities which must be specified in the model equations are the normalized observational error standard deviations. Table 1 depicts the observational errors currently being used. These errors are normalized by the forecast error, a field which evolves in space and time as the analysis/forecast system cycles on itself. This evolution is accomplished by adding an assumed forecast error growth rate to a field of analysis errors. By-products of the analysis, the analysis errors are statistical estimates of the error of interpolation and depend on the quantity, quality, and distribution of observational data.

The analysis proceeds from grid point to grid point until all points affected by data have been updated. For economy reasons no more than 10 pieces of data are allowed to influence any single grid point. The resulting analysis is a blend of prediction and observation; the weight of each depends upon the quality of the prediction and the quality, quantity, and distribution of observations.

Prediction

The NMC global model is a primitive equation prediction model with equations formulated in spherical geometry and solved on a regular latitude-longitude mesh with 2.5° resolution. The vertical structure of the atmosphere is resolved by nine layers, bounded by the earth's surface and the 50-mb level. The vertical coordinate is normalized pressure (σ); the atmosphere is divided into two "σ-domains" separated by a material surface tropopause. Figure 1 illustrates this vertical structure. There are three layers in the stratospheric domain and six in the tropospheric domain.

Prognostic variables in the model consist of potential temperature (θ), eastward (u) and northward (v) wind components, specific

Table 1. Observational errors assigned to different observation systems.

Temperature (°C)		Wind (m/s)	
Data Source	Error	Data Source	Error
Rawinsonde	0.8	Rawinsonde	1.5
Remote Sounding	2.0	Aircraft	2.0
		Cloud Winds	
		Low Level	3.0
		High Level	5.0

humidity (q), and pressure thickness of the tropospheric and stratospheric σ-domains. Potential temperature, wind, and specific humidity are defined at the midpoints of each layer. Diagnostic variables such as geopotential and vertical motion are calculated at the interfaces between layers. Physical processes included in the model are radiation, precipitation and evaporation, sensible heat exchange, and friction. The time integration scheme is a modification of the centered-difference method with a time filter.

Updating procedure

At 6-hour intervals the prediction model's history variables are updated by application of the statistical analysis procedure. The analysis is performed at the model grid points and in the prediction model's vertical coordinate, rather than on standard isobaric surfaces. Hence it is necessary to first update the mass field variables in order to redefine the vertical coordinate in which updates for the other variables are done. The mass variables are defined in terms of the model terrain pressure and the model tropopause pressure.

The terrain pressure analysis is a "D-value" analysis; departures of predicted model terrain pressure from standard atmosphere pressure are updated. This analysis is accomplished by a univariate, two-dimensional application of the statistical analysis procedure. Station pressure observations, if available, are used in the update. If station pressure is unavailable, mean sea level reports are used, provided station elevation is less than 500 m. Observations are converted to D-values by subtracting the standard atmosphere pressure corresponding to the station elevation. Observations are adjusted hydrostatically to the model elevation. An analysis of D-value corrections is performed

on the 2.5° mesh of the prediction model; the corrections are then combined with the guess field of D-values and smoothed with a spherical harmonic filter having 36 mode resolution. Adding standard atmosphere pressure at the model terrain elevation to each grid point D-value completes the update.

The next step in redefining the vertical coordinate is the analysis of tropopause pressure. Since the model requires a numerically well-behaved tropopause for stability, emphasis is placed on producing a tropopause with smooth spatial variation, strong climatological controls, and small variation from one update to the next. A univariate two-dimensional statistical analysis is performed on a 5° subset of the prediction mesh and interpolated to the 2.5° prediction grid using a spherical harmonic filter with 24 modes. Observational data consist of radiosonde reports of tropopause pressure and values of tropopause pressure calculated from remote soundings.

After completion of the surface pressure and tropopause pressure updates, the vertical coordinate is redefined and the original prediction variables are interpolated directly form midpoints of the old σ-layers to midpoints of the new σ-layers. After interpolation, the thermal, moisture, and rotational wind component fields are smoothed with the spherical harmonic filter with 36 modes in the troposphere and 24 modes in the stratosphere. The divergent wind component is truncated at mode 18 everywhere.

Next the layer-mean temperature and horizontal wind components are updated simultaneously by the complete multivariate, three-dimensional statistical analysis procedure described above. Residuals--differences between guess and observation--are interpolated to the midpoints of the nine layers in the updated vertical coordinate. Mass observations consist of observed thickness temperatures between standard isobaric levels for both radiosondes and remote soundings. Specific humidity residuals are analyzed univariately and only in the lowest five layers. This part of the analysis is performed on a 5° subset of the prediction mesh and interpolated to the remaining points of the mesh by the spherical harmonic filter. The filter has 36 modes for temperature, specific humidity, and the rotational component of wind in the troposphere and 24 modes in the stratosphere. The divergent component of wind is filtered everywhere at mode 18. Maps shown in Section 4 are produced at this point in the assimilation cycle by vertically interpolating the analyzed variables to standard pressure surfaces.

The updated fields are then initialized to suppress noise generated by the updating procedure. The initialization consists of a forward-backward time integration of the prediction model with a modification of the Euler-backward method. This integration is carried out for the equivalent of eight model time steps.

Finally the updated prediction is integrated forward in time for 6 hours to produce a guess for the next update. The statistical updating procedure is outlined in Figure 2 (a).

b. Spectral method

The operational analysis system, like the experimental system, updates predictions made by the NMC global model at 6-hour intervals.

Analysis

The spectral analysis system (Flattery, 1970) is basically a three-dimensional surface-fitting technique; observations are fit by least squares to surfaces described by series expansions of basis functions. Heights and winds are analyzed simultaneously. The longitudinal variation of height and wind component is described by trigonometric functions. The latitudinal variation of height is described by Hough functions, which arise in the solution of Laplace's tidal equation on a rotating sphere. The latitudinal variation of wind components is described by a special set of functions related to the Hough functions through the model wind law, which is very nearly geostrophic. Only rotational modes are used and hence the analyzed winds are nondivergent. This characteristic of the model is probably a disadvantage in the tropics where the divergent component of the wind can be rather large. The vertical variation of height and wind component is described by a set of orthogonal pressure functions derived empirically from current radiosonde and remote sounding data at 12-hour intervals. The analysis is done on constant pressure surfaces with a resolution of 24 horizontal modes and seven vertical modes.

The scheme is iterative, and the resolution is increased during each scan through the observations. Nine scans are performed in all, the last four at full resolution. The guess is not weighted in any systematic way. The analysis essentially replaces the guess with observations in areas where observations are present and retains the guess elsewhere.

Updating procedure

Beginning with predicted fields in the sigma vertical coordinate system of the prediction model, heights, winds, temperatures, and relative humidities are interpolated to standard isobaric levels at every point of the 2.5° mesh. These vertically-interpolated fields are then transformed (second step) to phase space by applying the analysis model with grid point values treated as observations. The wind law in enforced very weakly; thus the mass-motion balance of the prediction is approximately retained except that the divergent component of the forecast wind is removed. This step produces a set of guess coefficients that represents the prediction. Using the analysis procedure outlined above, the multivariate analysis of heights and winds (third step) is performed.

Relative humidity (fourth step) is analyzed for mandatory levels from 1000 to 300 mb. Three vertical functions are used and are not recalculated for each analysis.

Analyzed temperatures (calculated from analyzed heights) are used at grid points to locate the tropopause (fifth step), which is required by the model as a material surface. At each grid point the temperature profile is scanned vertically to locate a temperature minimum. The pressure corresponding to the temperature minimum constitutes the tropopause pressure (subject to latitudinally dependent pressure limits). Undefined tropopauses are assigned climatological default values. The resulting tropopause pressure field is filtered to remove small-scale variations.

Finally analyzed heights, temperatures, winds, and relative humidities are vertically interpolated to the prediction model's vertical coordinate. These fields constitute the initial state from which a 6-hour prediction is made. The spectral updating procedure is outlined in Figure 2 (b).

3. Description of Test

Each assmmilation system cycled for a period of 5½ days in the manner described in Section 2. Each began from the same guess at the beginning of the period and thereafter cycled independently of the other system. The time period covered was 1200 GMT 8 December to 0000 GMT 14 December 1977. Observations available to both systems include rawinsondes, remote soundings, satellite cloud-tracked winds, aircraft winds, and conventional land and ship surface observations.

Three-day predictions were made from the 0000 GMT 11 December analyses. The prediction model used is the NMC three-layer global model (Vanderman et al., 1976). The three-layer model is a primitive equation model similar in nature to the nine-layer model. The vertical coordinate is normalized pressure and consists of three equal $\Delta\sigma$ layers from model surface to 150 mb. Horizontal resolution is 3.75°. Since a vertical interpolation program was not available for interpolating directly from the nine-layer statistical analysis to the three-layer vertical coordinate of the prediction model, a double interpolation was performed. The statistical analysis was interpolated first to standard isobaric levels and then to the three-layer coordinate system. It is not known how much this double interpolation may have hurt the ensuing forecast. The spectral analysis underwent a single vertical interpolation from constant pressure directly to the three layers of the prediction model.

Each analysis valid at 0000 and 1200 GMT was verified against a network of tropical rawinsonde stations (Figure 3). All stations lie between 25°N and 25°S. Height, temperature, and wind were verified at 850, 500, 250, and 100 mb. Relative humidity was verified at 850 and 500 mb. The network consists of 131 stations, but on the average only about 90 of the 131 stations reported. Furthermore, several stations reported only wind. Since the statistical method performs its analysis in the prediction model's vertical coordinate, it was necessary to vertically interpolate the statistical analyses to constant pressure surfaces prior to verification.

A second means of objectively judging the quality of the analyses is by measuring the fit of each analysis to all data. This was done for thickness temperatures and winds for the tropical strip from 25°N to 25°S. Data were stratified by type (e.g., rawinsonde, aircraft, etc.) and pressure level. Only observations which failed to pass a gross error check were excluded from this verification.

The three-layer forecasts were verified in two ways for forecast hours 24, 48, and 72. The first way was against observations; each forecast was verified at 850, 500, and 300 mb against reports from the rawinsonde network shown in Figure 3. The second way was against analyses. This method was used only at 300 mb and only for winds. Each forecast was verified both against the statistical analysis and against the spectral analysis.

4. Results

a. Subjective comparison of analyses

Average zonal cross-sections of potential temperature and zonal wind in the tropics for the statistical and spectral analyses are shown in Figure 4. Each diagram represents an average of 11 analysis cases. The vertical coordinate is pressure. In general the two diagrams look very similar. Both depict a low-level easterly flow, which is strongest in the Northern Hemisphere, and a weak westerly flow which becomes stronger with increasing latitude, at higher levels. The temperature structure is very nearly the same between the two analysis systems in the low levels, but there are some differences at high levels. The vertical temperature gradient between 150 mb and 100 mb is stronger in the spectral cross-section near the equator. Due to the paucity of data in this region, it is difficult to say which analysis is more representative of the real atmosphere.

Tropical strip maps from a typical analysis are displayed in Figures 5, 6, and 7. Three levels--850, 500, and 250 mb--are shown for both analysis systems. Dashed lines are isotachs in knots. Plotted satellite observations of temperature and cloud-tracked wind are denoted by a star, rawinsonde observations by a circle, and aircraft observations by a square. Plotted wind vectors with no symbol attached are analyzed grid point winds.

In general the two analyses have represented the tropical atmosphere in about the same way. Both analyses appear to be reflecting most observations in a reasonable manner. The low level flow pattern is characterized by a well defined easterly flow in both the Atlantic and Pacific. A series of anticyclones flanks this belt of easterlies on the north and south. The easterlies are well defined by cloud-tracked winds which are not plotted because they are slightly below the 850 mb level. Some fairly large differences do exist between the two analyses, usually in data sparse areas. For example, the anticyclone over South America in the statistical analysis is barely hinted at in the spectral analysis. There are no observations in this area.

The 500 and 250 mb levels are less well defined than the 850 mb level. At 250 mb, several troughs in the Northern Hemisphere westerly flow extend well into tropical latitudes. One area of strong cross-equatorial flow is depicted between 30^{o}W and 40^{o}W longitude (Figure 7(a) and (b)). Several aircraft and cloud-tracked winds indicate that the statistical analysis has represented the wind speeds somewhat better, although both analyses have analyzed wind speeds slightly too weak. Figure 8 shows an expanded view of this area.

Two systematic differences in the way winds are analyzed at mid and high latitudes also appear to be in evidence at tropical latitudes. The first difference is that the statistical analysis appears to analyze for stronger wind speeds in areas where relatively strong wind reports are present. The above example of cross-equatorial flow is one example. A second example appears in the southwesterly flow around 20^{o}N, 20^{o}W (Figure 8). The statistical analysis usually analyzes such cases better than the spectral analysis. The slow bias of the spectral analysis has been traced in large part to the double vertical interpolation that must be performed between prediction model and analysis model coordinates each time an analysis is performed. The statistical method avoids such double vertical interpolations by performing the analysis in the prediction model's vertical coordinate.

The second difference occurs in areas of sharp curvature in the flow pattern. In such areas the spectral analysis produces winds which are overly geostrophic; the analyzed winds tend to be super-gradient in cyclonic flow, and sub-gradient in anticyclonic flow. An example can be seen at 250 mb in the base of the trough between 20^{o}N and 30^{o}N over Africa.

Figure 9 shows an expanded view of this area. The wind speed is about 20 knots weaker in the statistical analysis. There are no observations to judge which analysis is more correct, but other cases have shown that the statistical analysis usually handles such situations more correctly.

Fields of horizontal divergence were generated for the statistical analysis at several isobaric levels. This was not done for the spectral analysis since it is a nondivergent analysis. A small portion of the 250 mb divergence field is shown in Figure 10. The divergence field appears qualitatively reasonable. For example, a center of divergence appears near 7^{o}S, 70^{o}W where several cloud-tracked winds appear to define a diverging wind field (Figure 8).

A typical analysis of mean relative humidity is shown in Figure 11. The date is 1200 GMT 12 December. Figure 11(a) is the statistical analysis, Figure 11(b) the spectral analysis. Relative humidity has been averaged over the first four sigma layers of the model. Areas exceeding 90% are cross-hatched. The most striking difference between the two analyses is that the statistical analysis is much drier in tropical latitudes. There are no humidity observations available in the Pacific in the large area on the spectral analysis which exceeds 90%. Similarly, there are no observations available in those tropical areas of the Atlantic where the spectral analysis exceeds 90%. At several points north and south of the 90% band in the Pacific, observations are available and appear to be analyzed for fairly well (e.g., Guam, Wake, and Hilo on the north, and Pago Pago on the south). All observations near the 90% area have average relative humidities from surface to 500 mb of less than 90%. It is therefore difficult to believe that the tropical Pacific is really as moist as the spectral analysis depicts. A similar argument can be made in the Atlantic where again only data void areas exhibit relative humidities in excess of 90% in the spectral analysis. It appears then that the difference between the two analyses is due in large measure to a wet bias in the spectral analysis. It is possible that part of the difference could be due to a dry (but smaller) bias in the statistical analysis. Similarly large differences occur at other analysis times.

b. Statistical comparison of analyses

Each of the analyses valid at 0000 and 1200 GMT was verified against observations from the rawinsonde network of Figure 3 in order to detect systematic differences in the way the data are fit. Results for four-levels--850, 500, 250, and 100 mb--and for three variables--height, temperature, and wind--are depicted in Figure 12. Both root-mean-square (RMS) and average (AVG) scores are shown and are averaged for 12 analysis cases.

Looking first at the RMS scores, the statistical analysis fits the observations more closely for all variables at 500 and for all variables except wind at 100 mb. At 850 mb the spectral analysis fits the data more closely for all variables except winds. At 250 mb heights are fit more closely by the statistical analysis, winds less closely, and temperatures virtually the same as the spectral. Generally speaking the differences are small. The relatively poor fits at 850 mb by the statistical analysis may be a result of not using surface reports in the upper-air analysis. Surface reports are used only in the surface pressure analysis at the present time. A future modification will incorporate these reports in the multivariate upper-air analysis. The relatively poor wind fit at 250 mb by the statistical method may be the result of assuming a prediction error growth rate which is too small (thus giving the prediction too much weight), or it may be the result of excessive smoothing by the spectral filter.

The magnitudes of average height errors are smaller for the statistical analysis at all levels except 100 mb where both systems exhibit a rather large negative bias. Average temperature errors are smaller in magnitude for the statistical analysis at all levels except 850 mb. Average wind errors are small and negative (winds too weak) for both methods.

Figure 13(a) shows average and RMS fits of analyzed relative humidity to the same set of stations as Figure 12. At 850 mb the RMS scores are nearly identical between the analysis systems. At this level the spectral analysis exhibits a small wet (positive) bias, whereas the statistical analysis has a substantially larger dry (negative) bias. At 500 mb the statistical analysis has a much better RMS score and no bias. The spectral analysis shows a wet bias.

If the spectral analyses are excessively wet in data void areas, as was argued earlier, one would expect the ensuing forecasts made from those analyses to exhibit a wet bias. In other words, moisture in data void areas might be expected to spread, during the course of the forecast, to the verification stations. Figure 13(b) depicts the average bias of the six-hour predictions made from the two analysis systems. Only those forecasts valid at 0000 and 1200 GMT are included in the statistics (11 cases). As expected, the predictions made from spectral analyses show a rather large wet bias.

The two analyses are next verified against all thickness temperature and wind observations within a ± 3 hour time window of the 0000 and 1200 GMT synoptic times. Observations are stratified by data type. Thickness temperature fits are presented in Figure 14, wind fits in Figure 15. Cloud-tracked winds and aircraft winds are placed, without adjustment, at the nearest standard isobaric level. Hence some of these

observations are slightly off-level. Cloud-tracked winds and aircraft winds are not available at all four levels verified. Thickness temperatures are for the standard isobaric layer immediately above the levels indicated in Figure 14.

Since the statistical method analyzes thickness temperatures directly, one might expect it to fit such observations better than the spectral method, which analyzes heights rather than thickness temperature. Such is the case for both remote soundings and radiosondes for all layers shown except the 250-200 mb layer. The reason for this inconsistency is not known, but it appears that some adjustment to the statistical procedure may be in order. Perhaps the assumed error growth rate of the predictions is unrealistically small, allowing too little weight of data compared to forecast.

Figure 15 shows that the statistical analysis fits the wind data less well at 250 mb for all data types than does the spectral analysis. This result is consistent with the radiosonde verification of Figure 12(c). As was stated earlier, the relatively larger errors may be a result of a prediction error growth rate which is too small or the spectral filter may be smoothing the wind field excessively. Reanalysis of two cases suggests that most of the error difference can be made up by increasing the filter resolution slightly. At other levels the statistical wind analyses verify slightly better than the spectral analyses.

c. Statistical verification of three-layer forecasts

Verification statistics for the three-layer forecasts are shown in Figures 16 and 17. Figure 16 is a verification against rawinsonde data, Figure 17 against analyses. The data verification was done at three levels--850, 500, and 300 mb--with data from the same set of stations (Figure 3) as used for analysis verification. Overall the forecast made from the statistical analysis verifies worse at 850 mb and better at 300 mb for all variables. At 500 mb the two forecasts verify about the same. The relatively poor forecast at 850 mb by the prediction from the statistical analysis may be a result of not using surface data in the upper-air analysis. However, it is difficult to draw conclusions from a single forecast case.

Verifications against analyses were performed only at 300 mb and only for winds. The verifications (Figure 17) are somewhat sensitive to the choice of verifying analysis. When the spectral analysis is used for verification, the two forecasts have about the same error; the spectral initialized prediction is slightly better at 24 hours but slightly worse at 48 and 72 hours. When the statistical analysis is used for verification, the statistical initialized prediction makes smaller errors at all forecast times. It is encouraging to note that both forecasts score better than persistence at all forecast hours.

5. Summary

The performance of the NMC statistical analysis system has been compared with the NMC operational spectral system at tropical latitudes. Some design advantages of the statistical system in the tropics include retention of a smoothed divergent wind component and a systematic data weighting scheme. Generally speaking the two analysis systems performed about equally well for a 5½ day test period in December 1977. Some systematic differences were found. Spectral moisture analyses were found to have a wet bias. Variables which were found to have larger errors in the statistical analyses include 250 mb winds, 850 mb heights and temperatures, and thickness temperatures for the 250 to 200 mb layer. Some minor adjustments in the assimilation system may be desirable to reduce these errors.

A three-day prediction made from a statistical analysis compared favorably with one made from the corresponding spectral analysis. Both forecasts succeeded in bettering persistence out to and including 72 hours.

REFERENCES

Bergman, K. H., 1976: Multivariate objective analysis of temperature and wind fields using the thermal wind relationship, Preprints, Sixth Conf. on Weather Forecasting and Analysis, May 10-13, 1976, Albany, N.Y. (AMS), 187-190.

_____ and D. Gordon, 1977: Spatial correlation of forecast errors and climatological variances for optimum interpolation analysis. Preprints, Fifth Conf. on Probability and Statistics in Atmospheric Sciences, Nov. 15-18, 1977, Las Vegas, Nev. (AMS), 79-84.

Flattery, T. W., 1970: Spectral models for global analysis and forecasting, Proc. Sixth AWS Technical Exchange Conf., U.S. Naval Academy, Annapolis, Md., Air Weather Service Tech. Rpt. 242, 42-54.

Gandin, L. S., 1963: Objective analysis of meteorological fields. Gidrometeorologicheskoe Isdatel'sto (GIMIZ),Leningrad, (Israel Program for Scientific Translations, Jerusalem, 1965, 242 pp.).

Stackpole, J. D., 1976: The National Meteorological Center 9-layer global forecast model, Preprints, Sixth Conf. on Weather Forecasting and Analysis, May 10-13, 1976, Albany, N.Y. (AMS).

Vanderman, L. W., J. F. Andrews and J. F. O'Connor, 1976: Extended period forecasting with a global three-layer primitive-equation model, National Weather Digest, vol. 1, No. 1, 13-24.

$$\sigma_s = \frac{p - p_{10}}{p_7 - p_{10}}$$

$$\sigma_T = \frac{p - p_7}{p_1 - p_7}$$

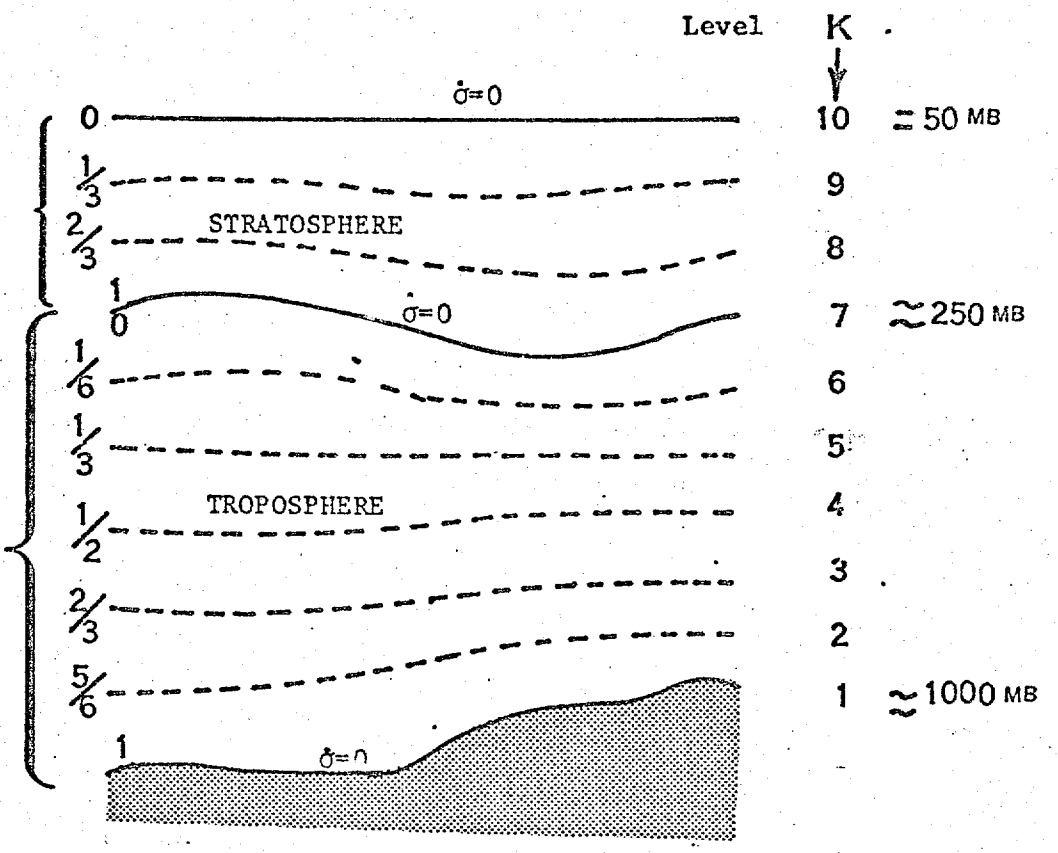

Fig. 1 Schematic Diagram of the vertical structure of the nine-layer model.

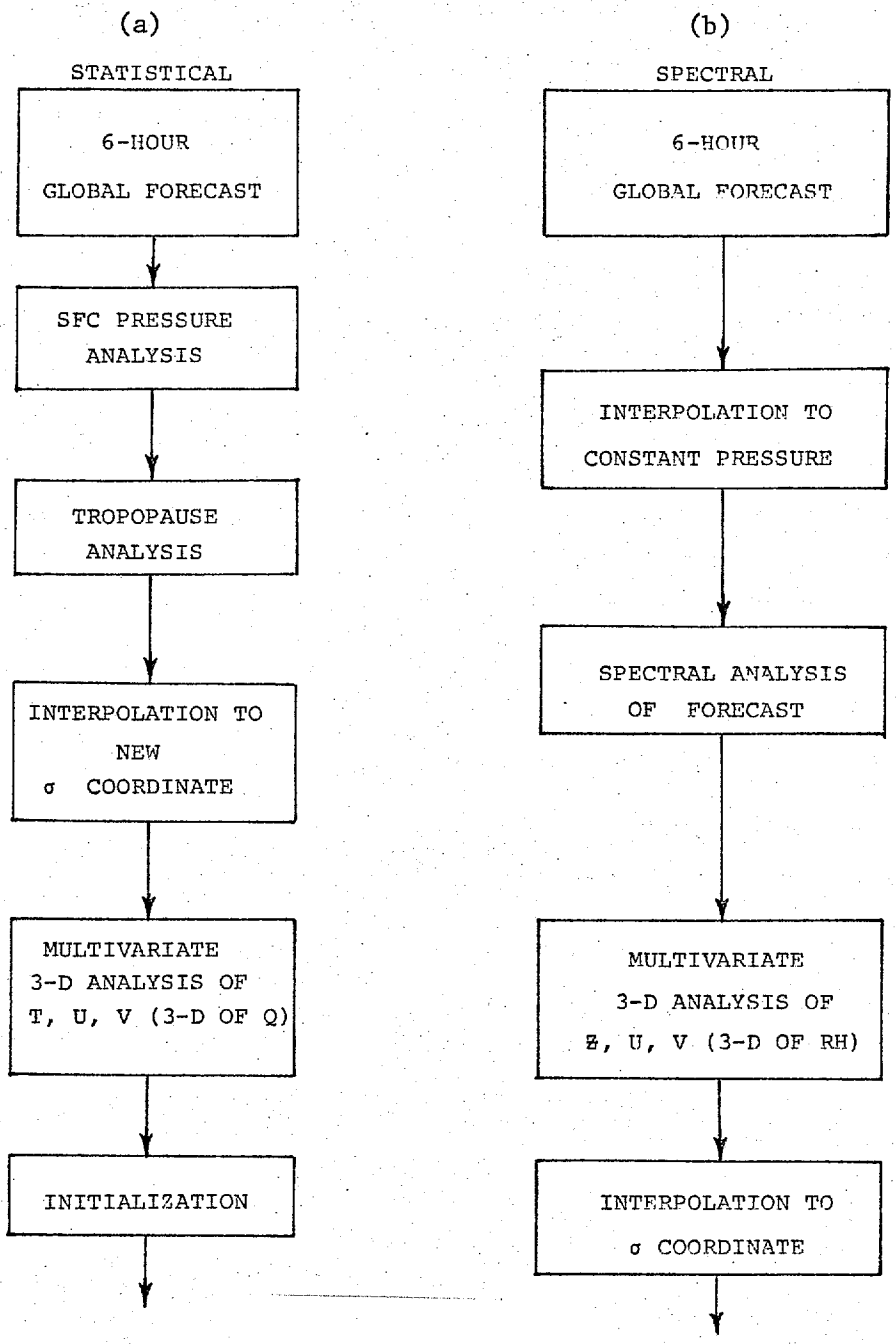

Fig. 2 Major Updating Steps.

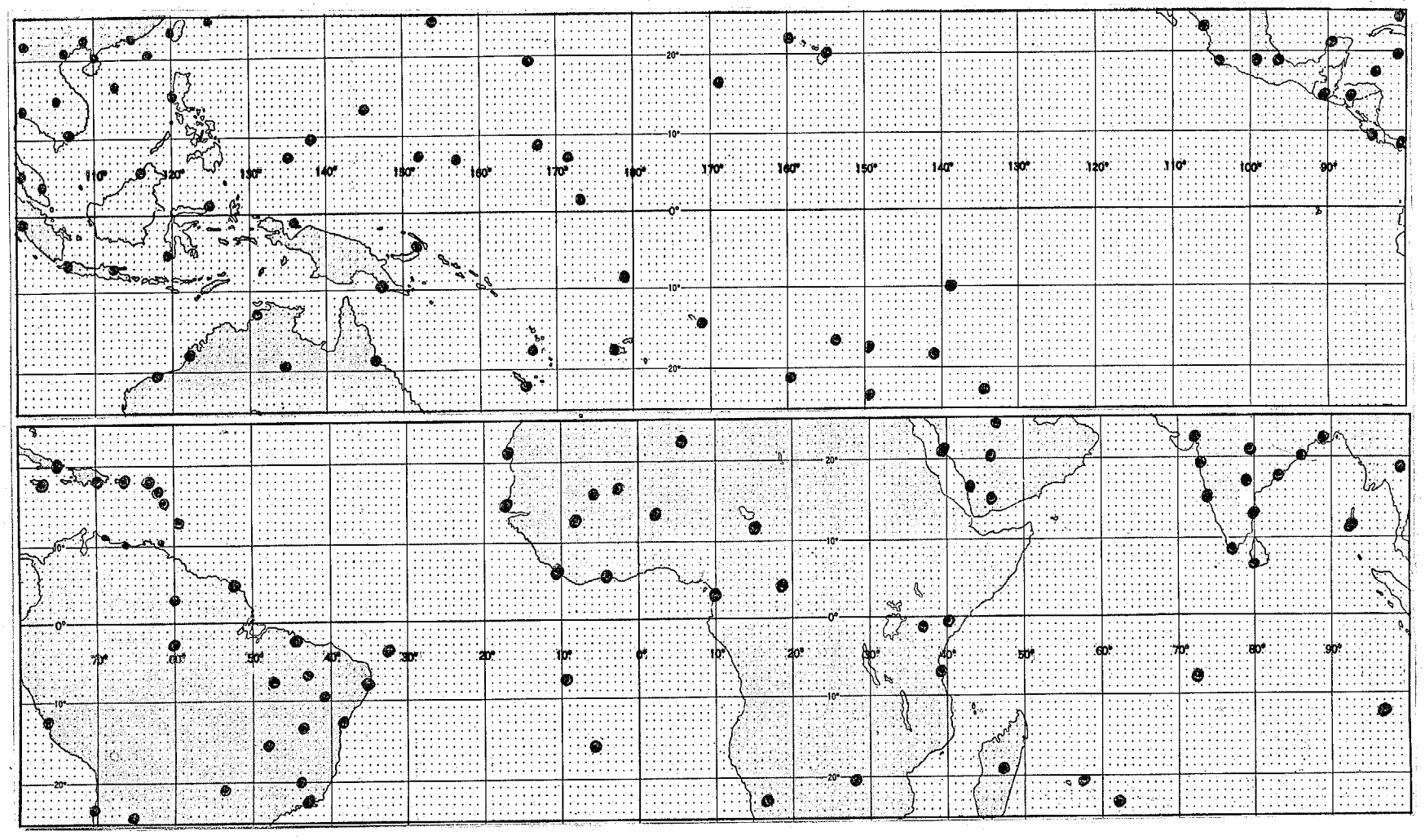

Figure 3. Rawinsonde verification network.

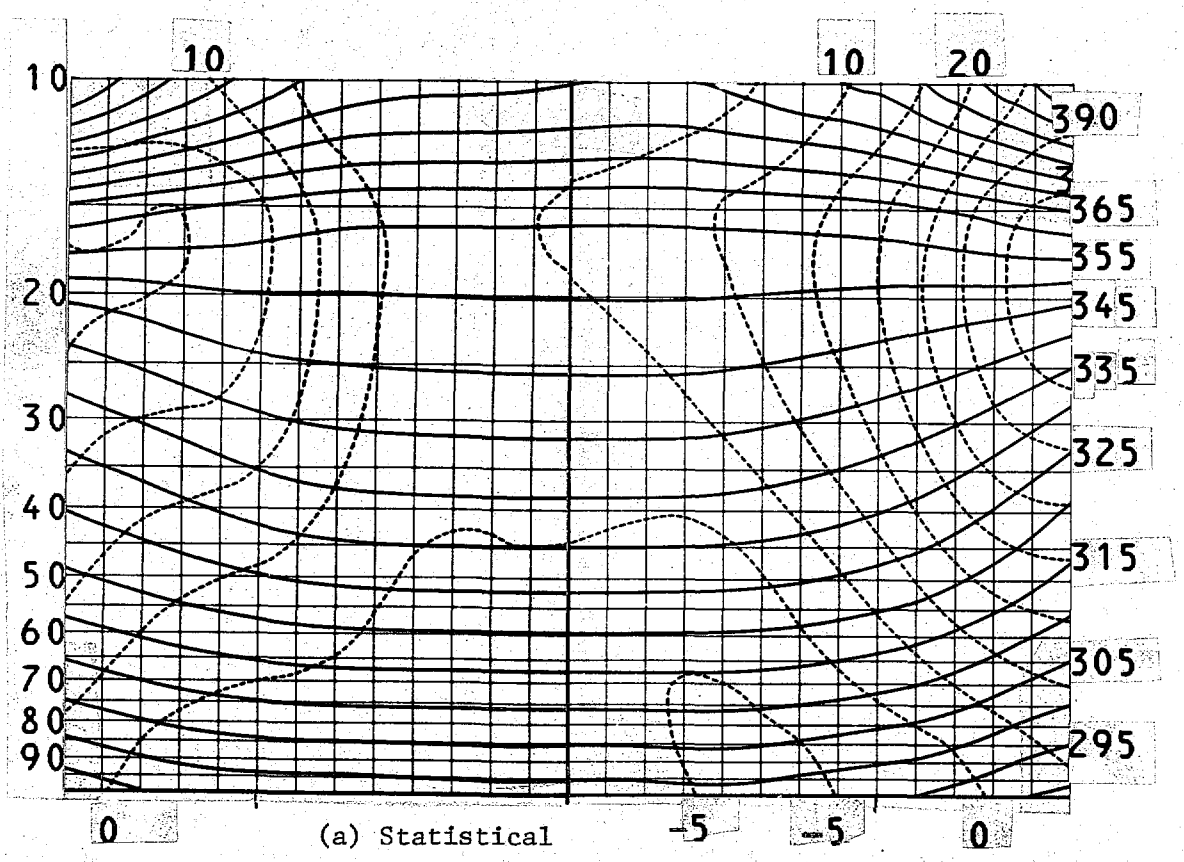

(a) Statistical

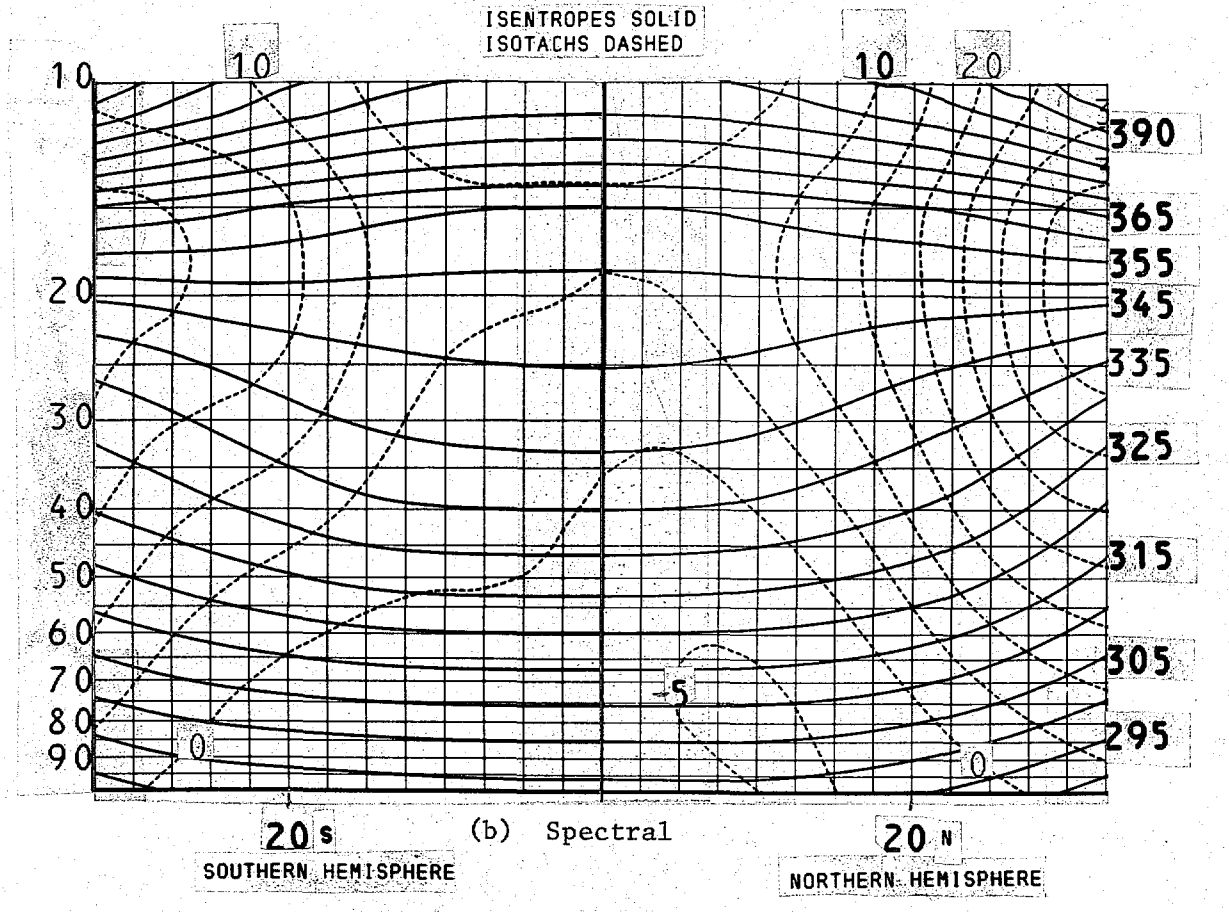

(b) Spectral

Figure 4. Analysis zonal cross-sections averaged over 11 cases, 1200 GMT 8 December to 0000 GMT 14 December 1977

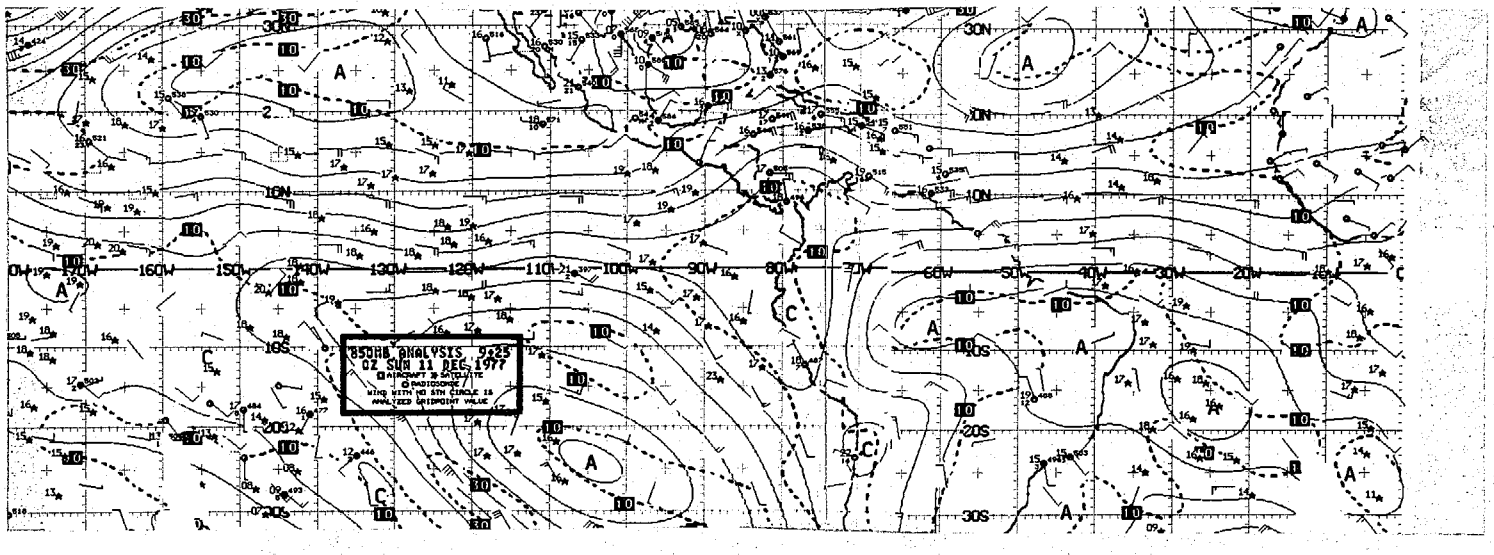

(a) Statistical - Western Hemisphere

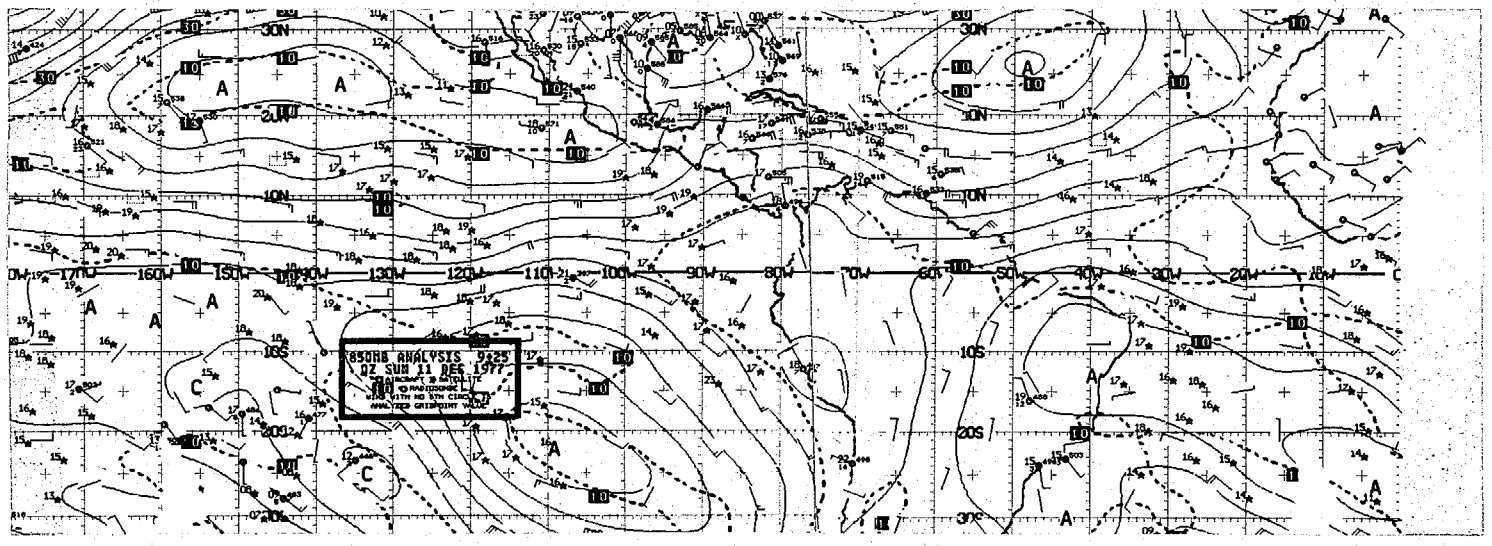

(b) Spectral - Western Hemisphere

Figure 5. 850 mb analysis.

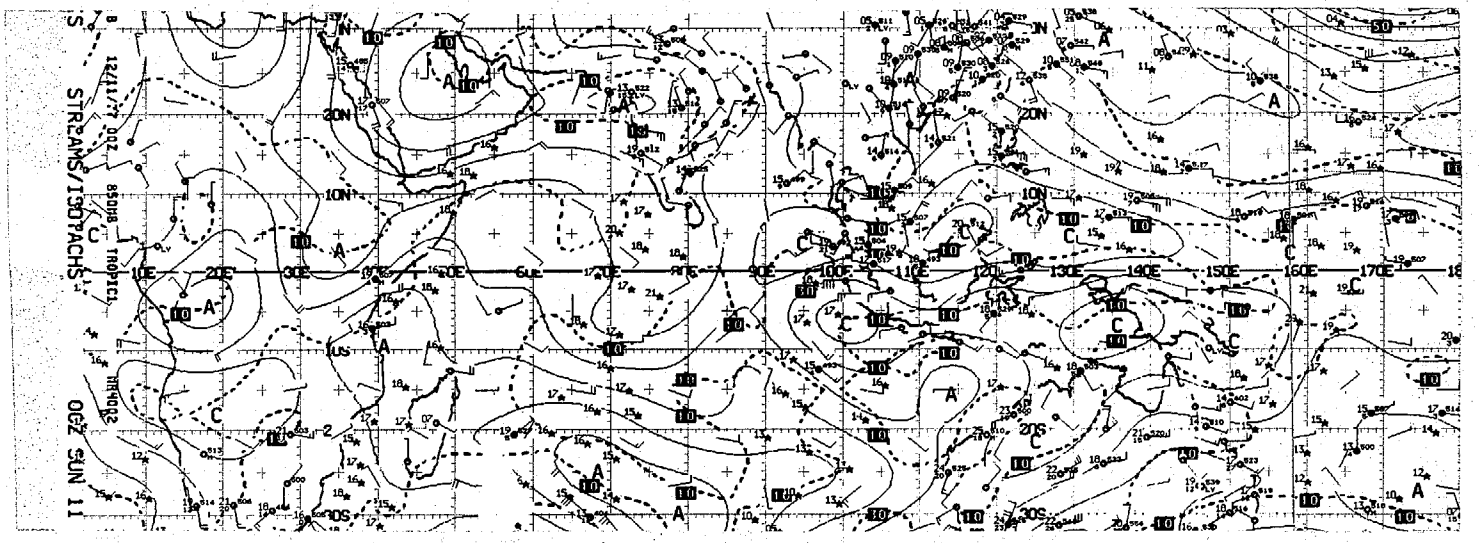

(c) Statistical - Eastern Hemisphere.

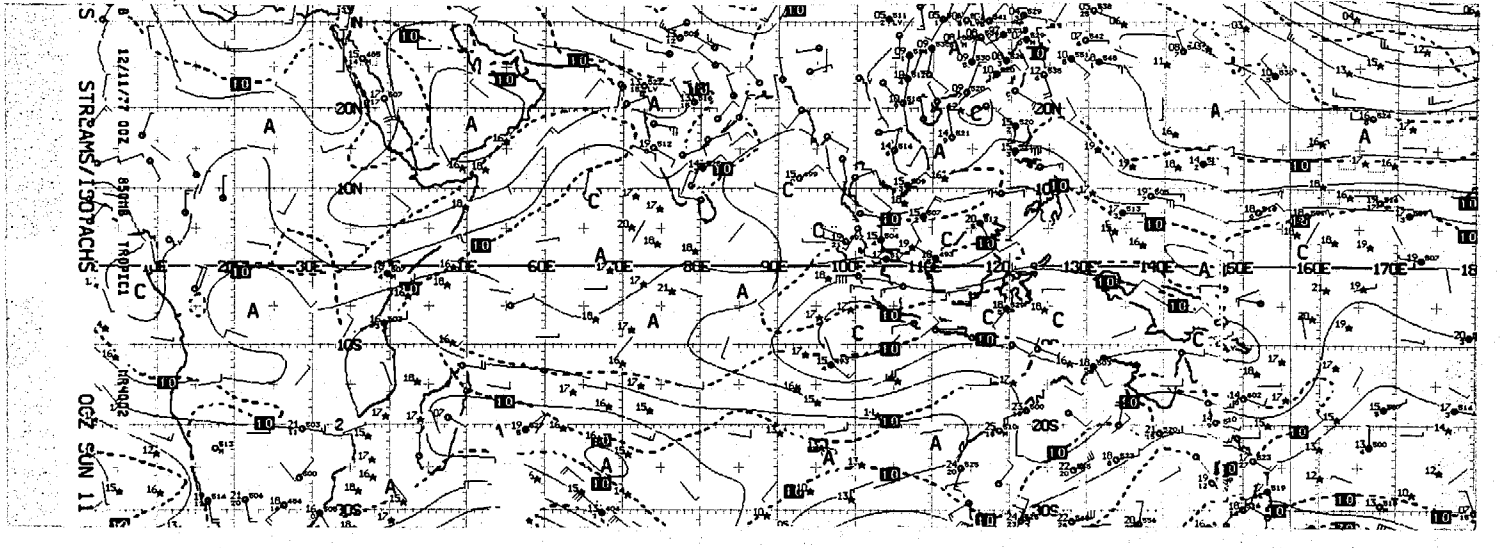

(d) Spectral - Eastern Hemisphere

Figure 5. (continued)

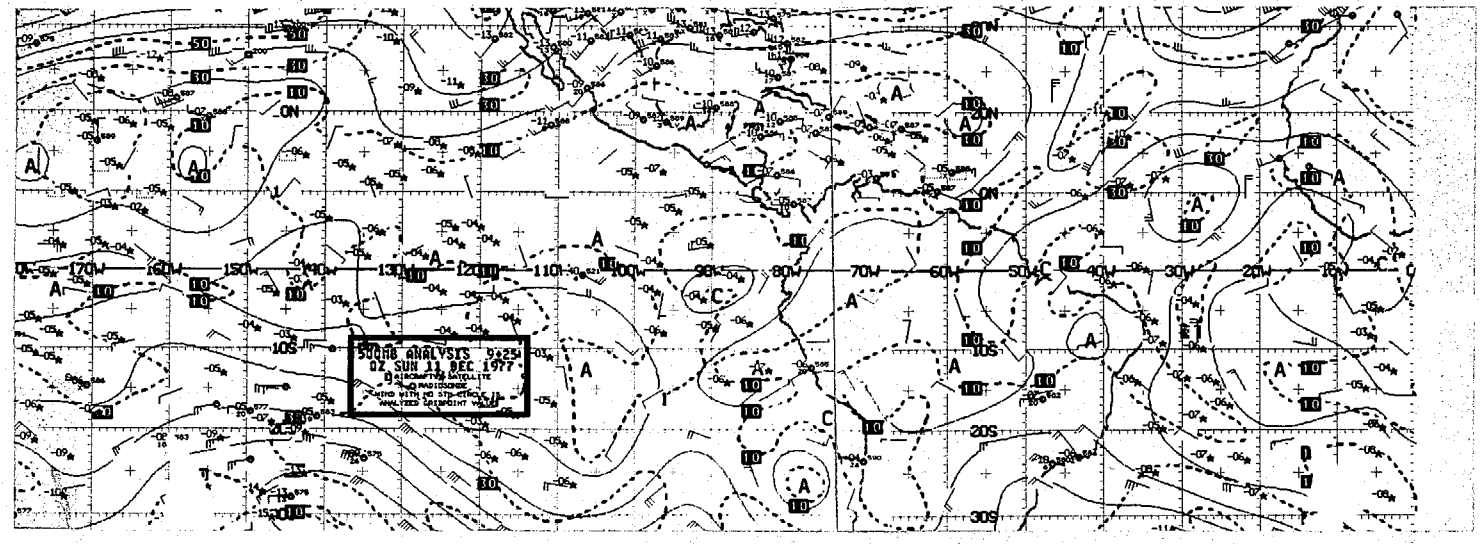

(a) Statistical - Western Hemisphere

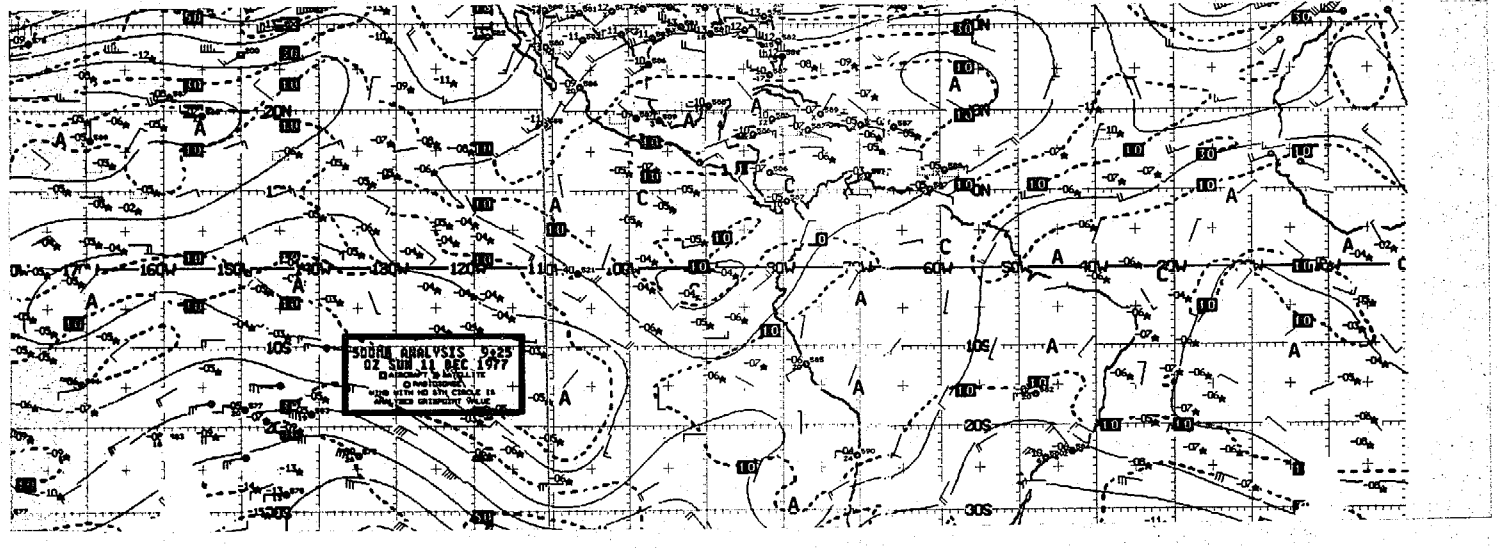

(b) Spectral - Western Hemisphere

Figure 6. 500-mb analysis

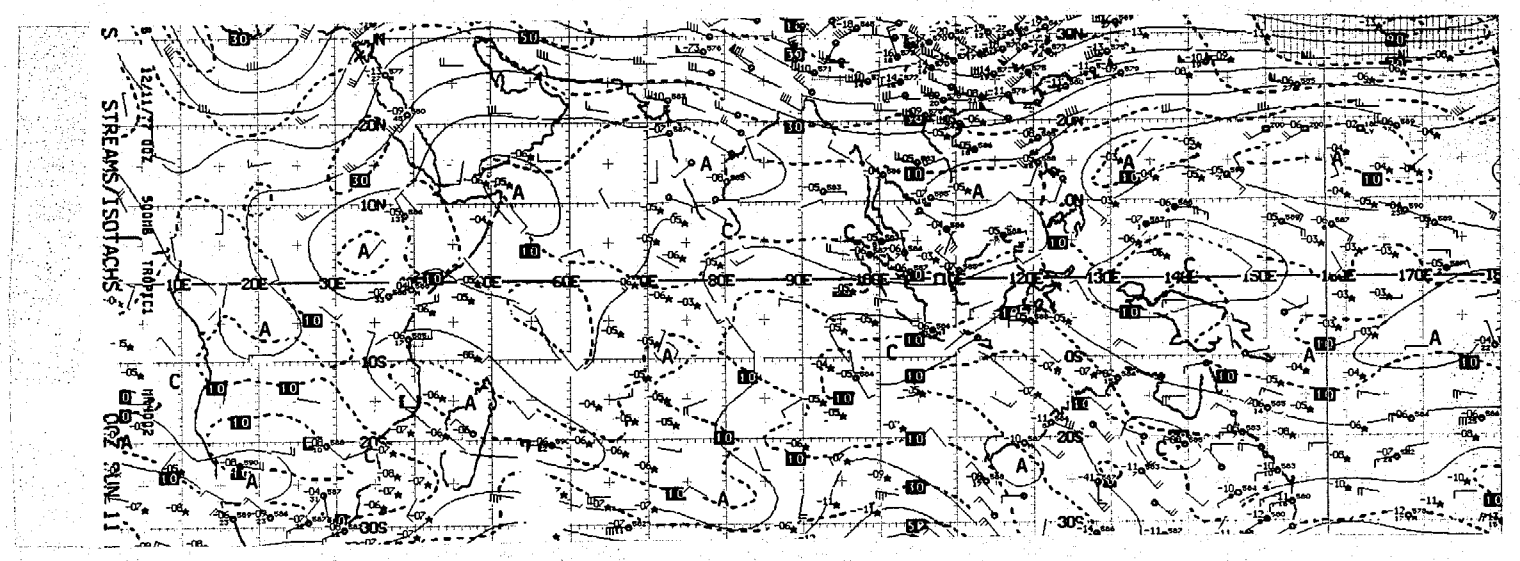

(c) Statistical - Eastern Hemisphere

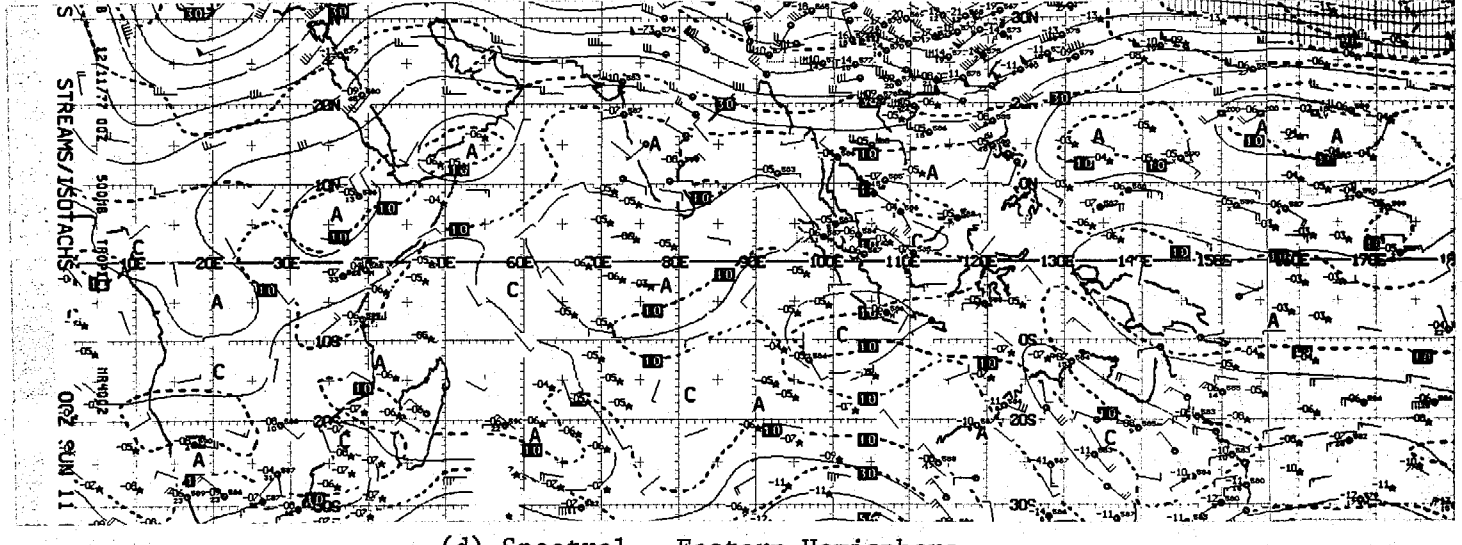

(d) Spectral - Eastern Hemisphere

Figure 6. (continued)

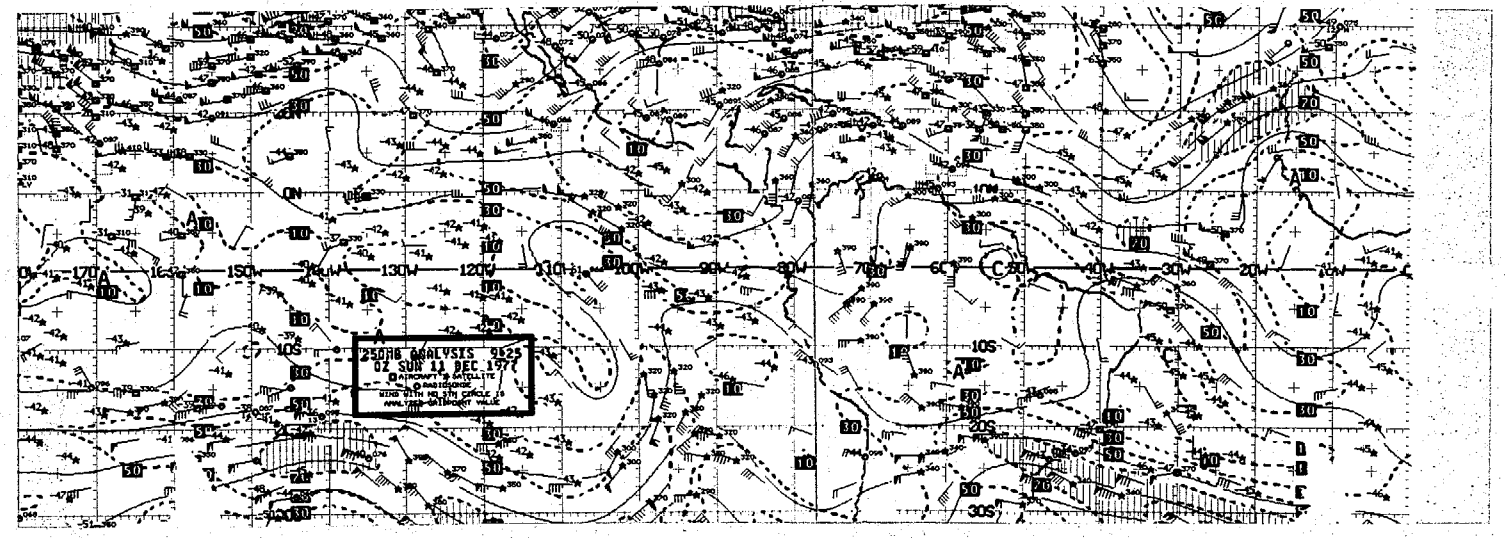

(a) Statistical - Western Hemisphere

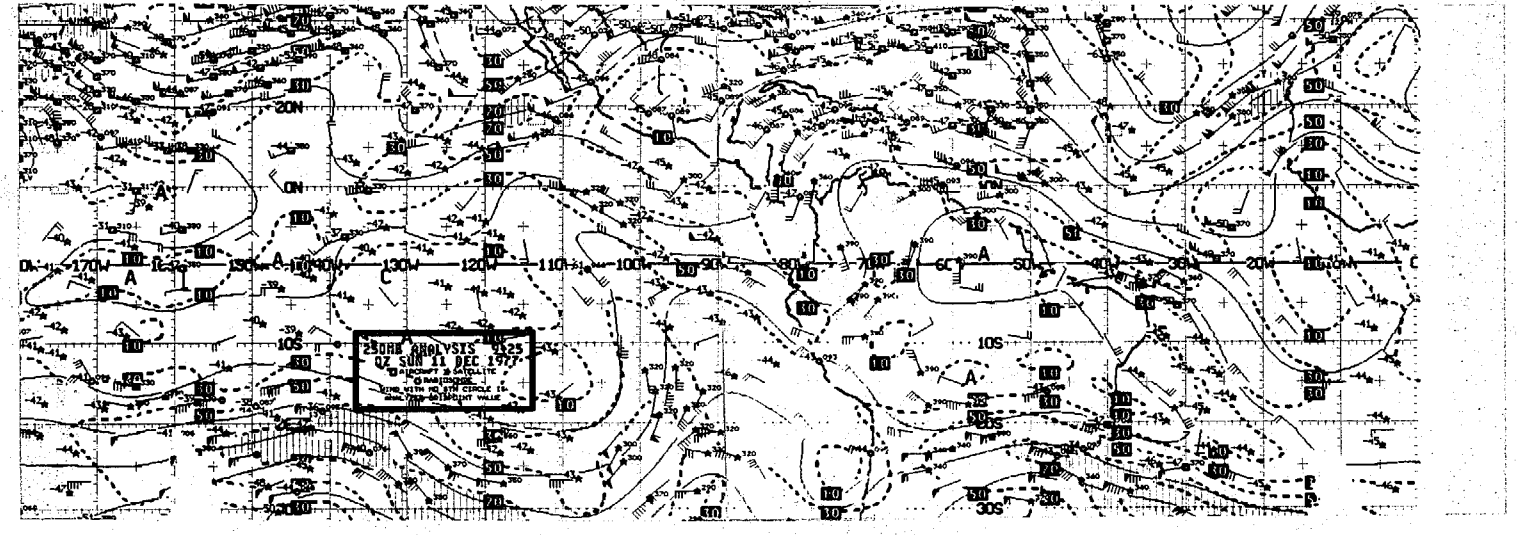

(b) Spectral - Western Hemisphere

Figure 7. 250-mb analysis

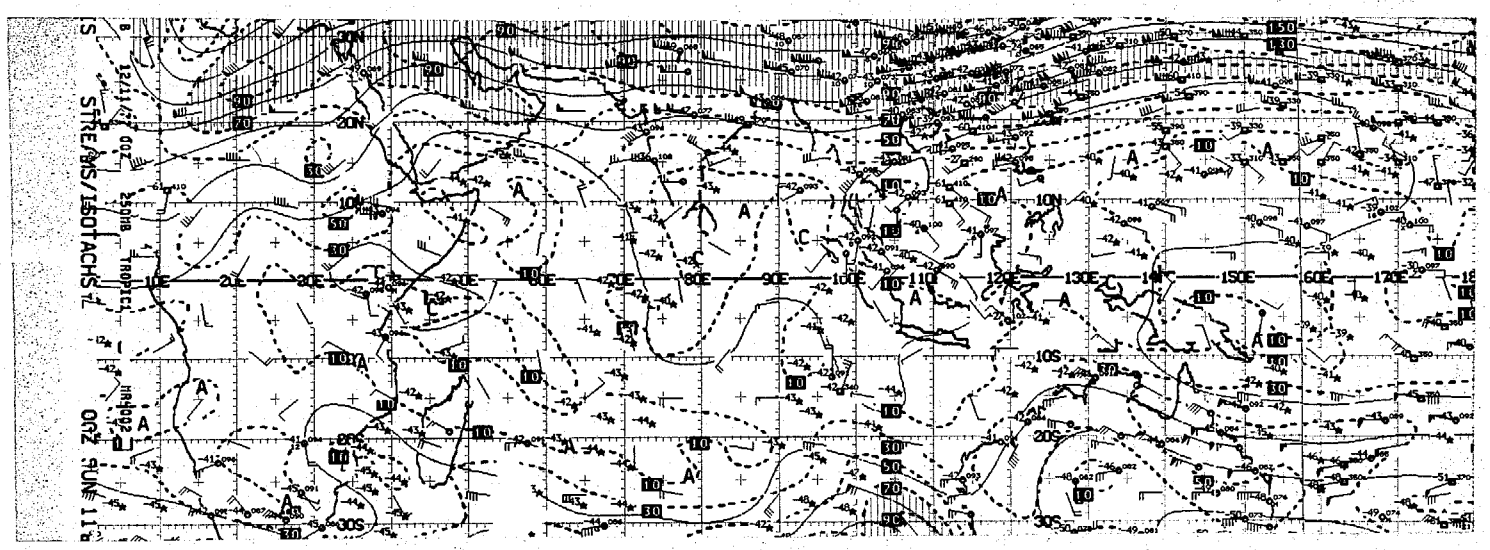

(c) Statistical - Eastern Hemisphere.

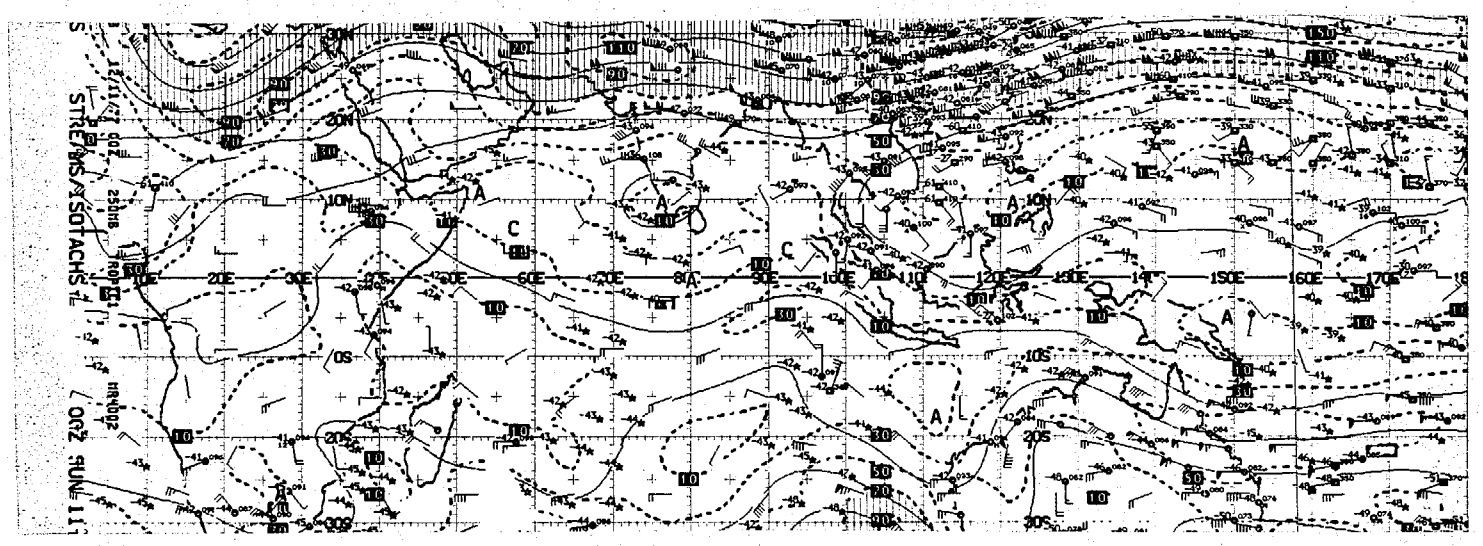

(d) Spectral - Eastern Hemisphere.

Figure 7. (continued)

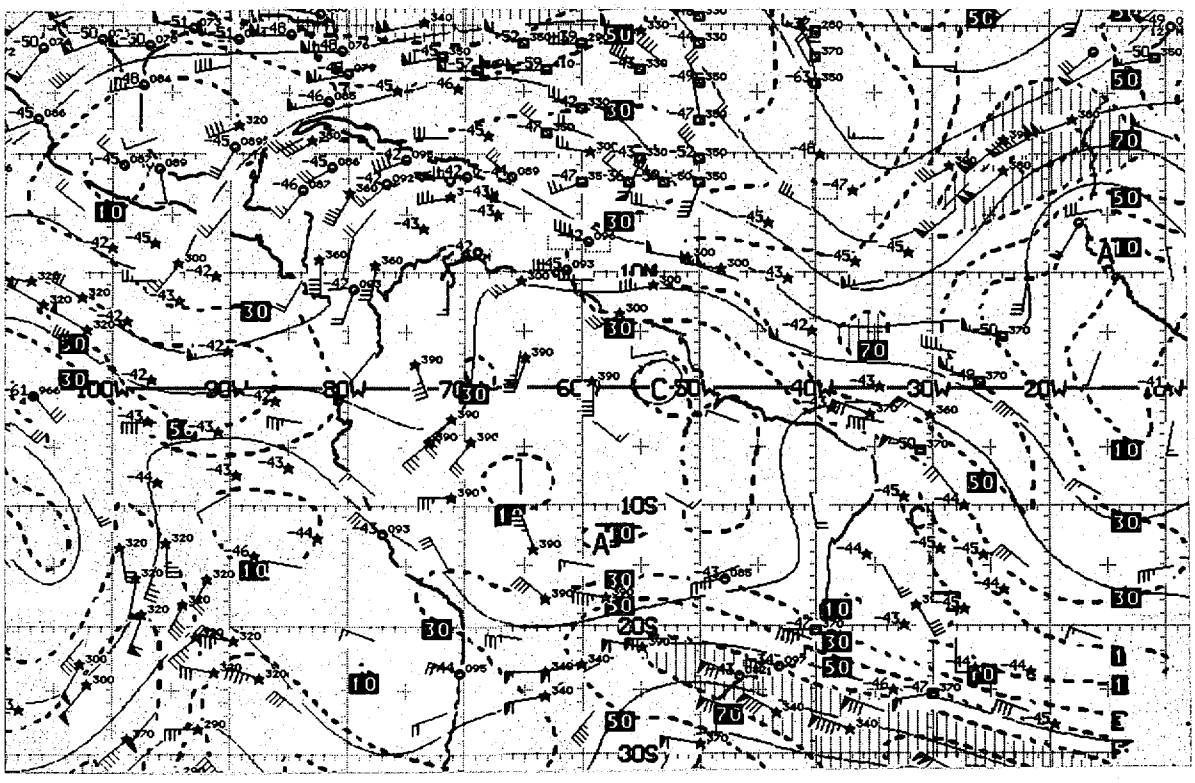

(a) Statistical

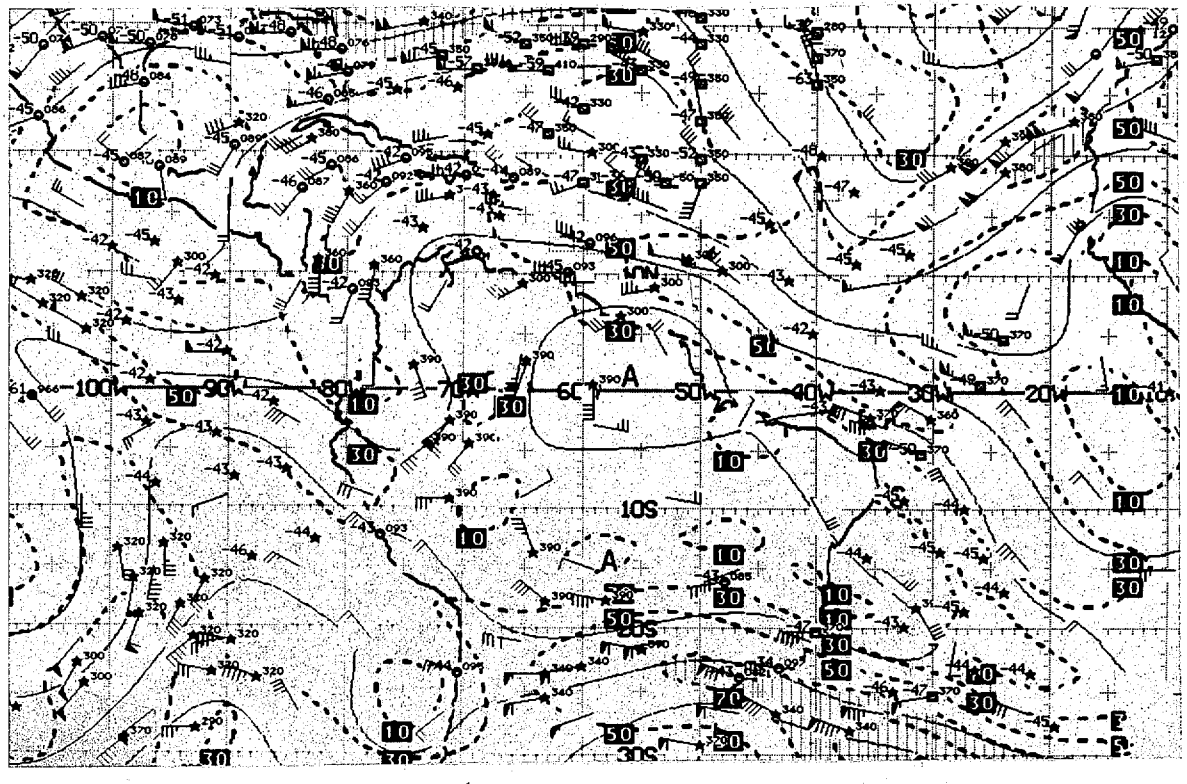

(b) Spectral

Figure 8. 250-mb analysis, 0000 GMT 11 December 1977

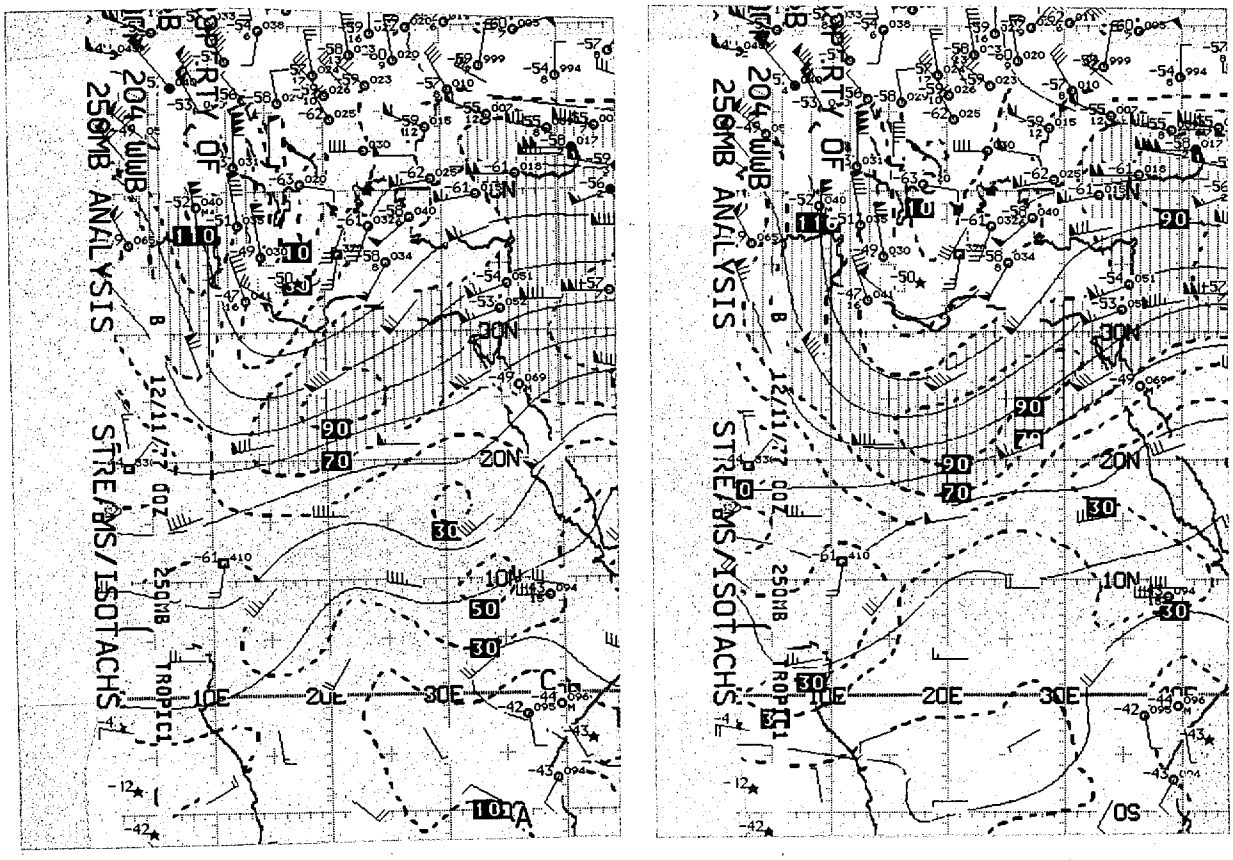

(a) Statistical

(b) Spectral

Figure 9. 250 mb analysis, 0000 GMT 11 December 1977.

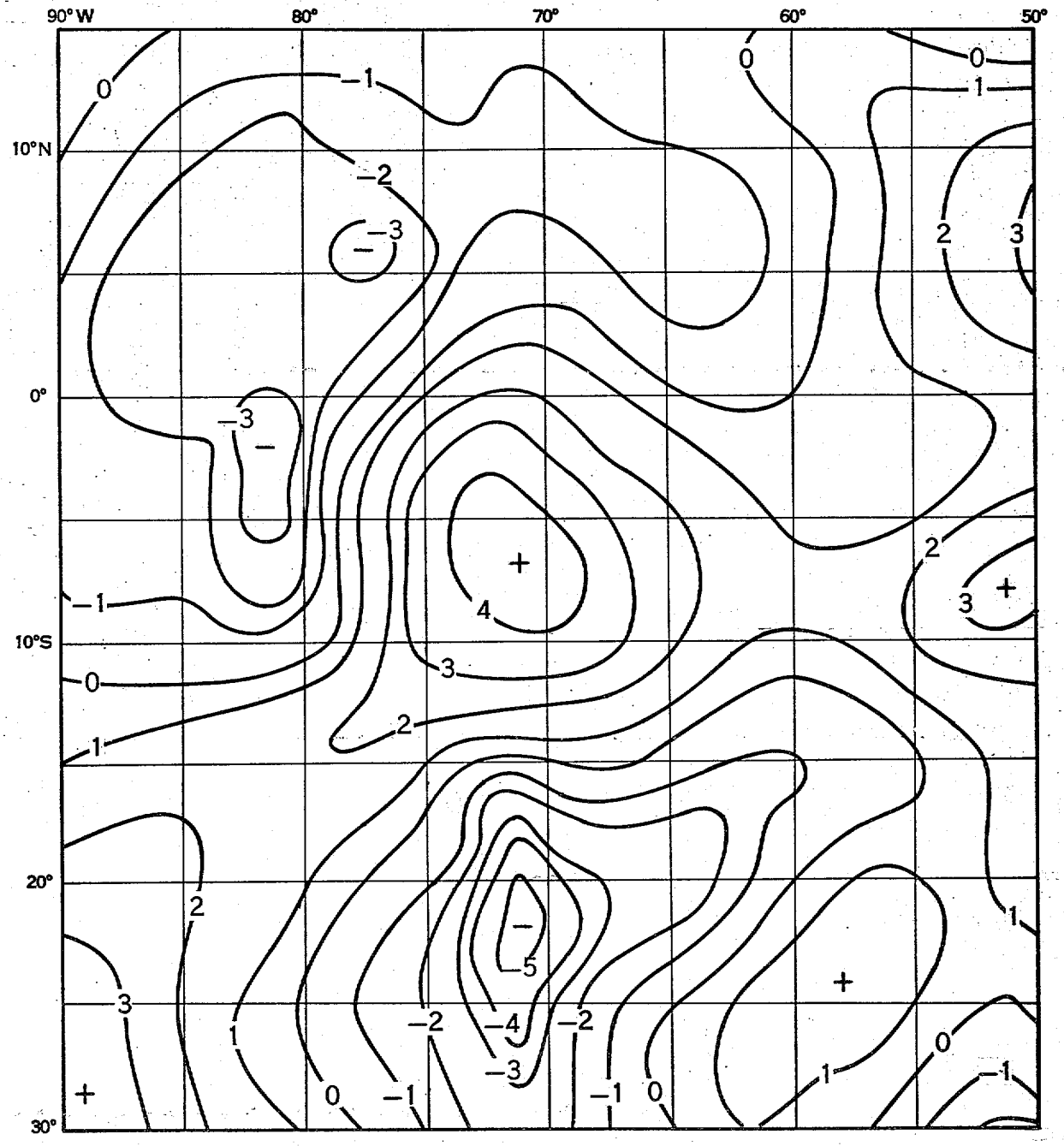

Figure 10. 250-mb horizontal divergence ($xr^2 \times 10^{-8}$ m^2/s) from 0000 GMT 11 December 1977 statistical analysis. r = earth's radius (m).

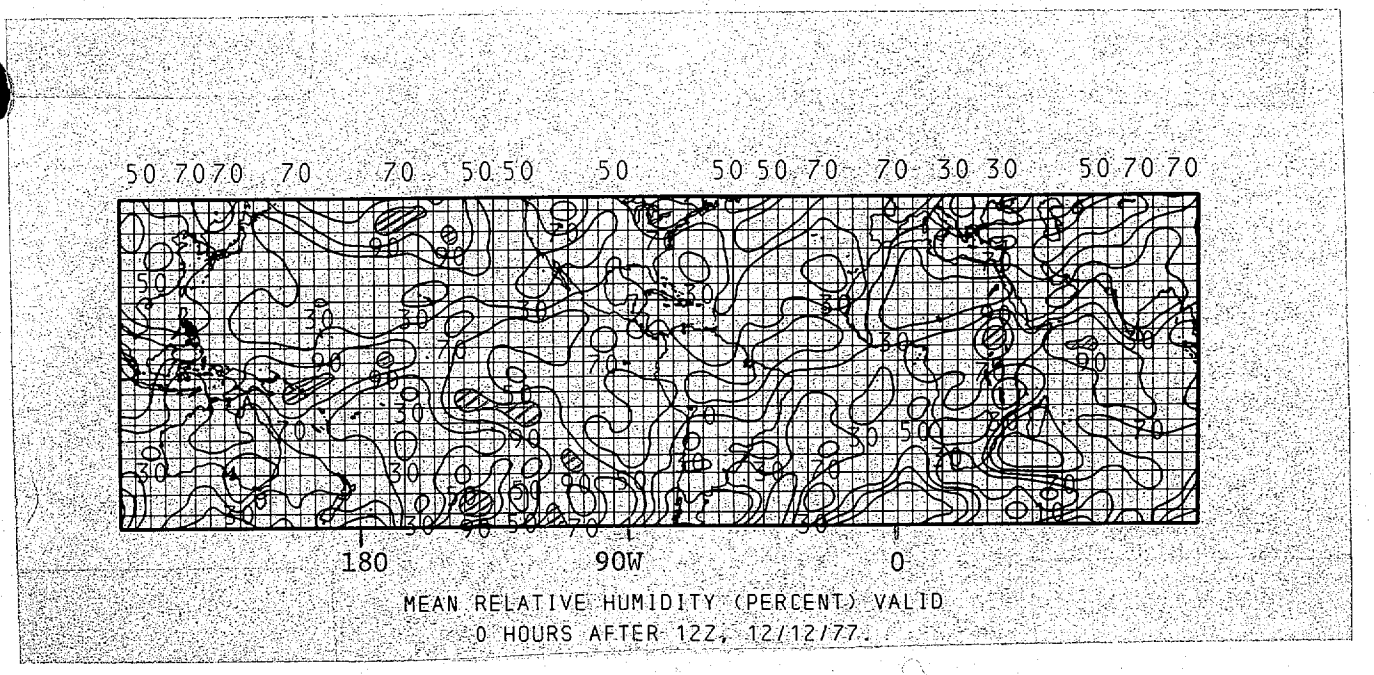

(a) Statistical

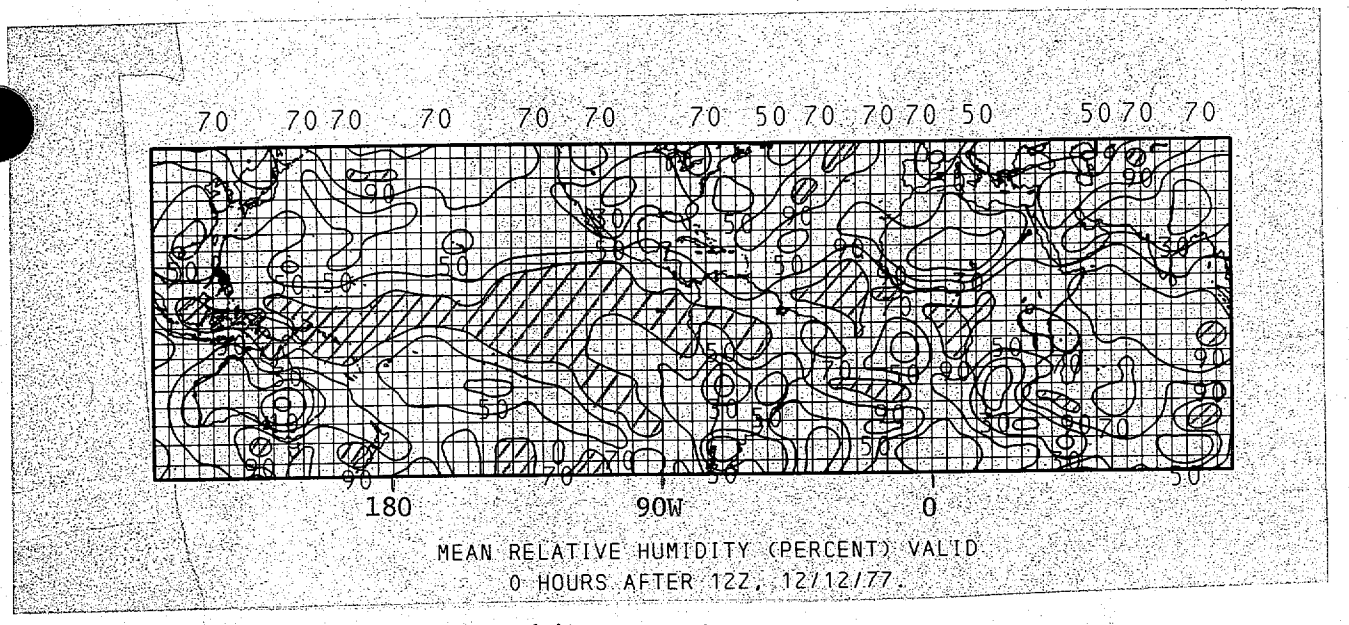

(b) Spectral

Figure 11.

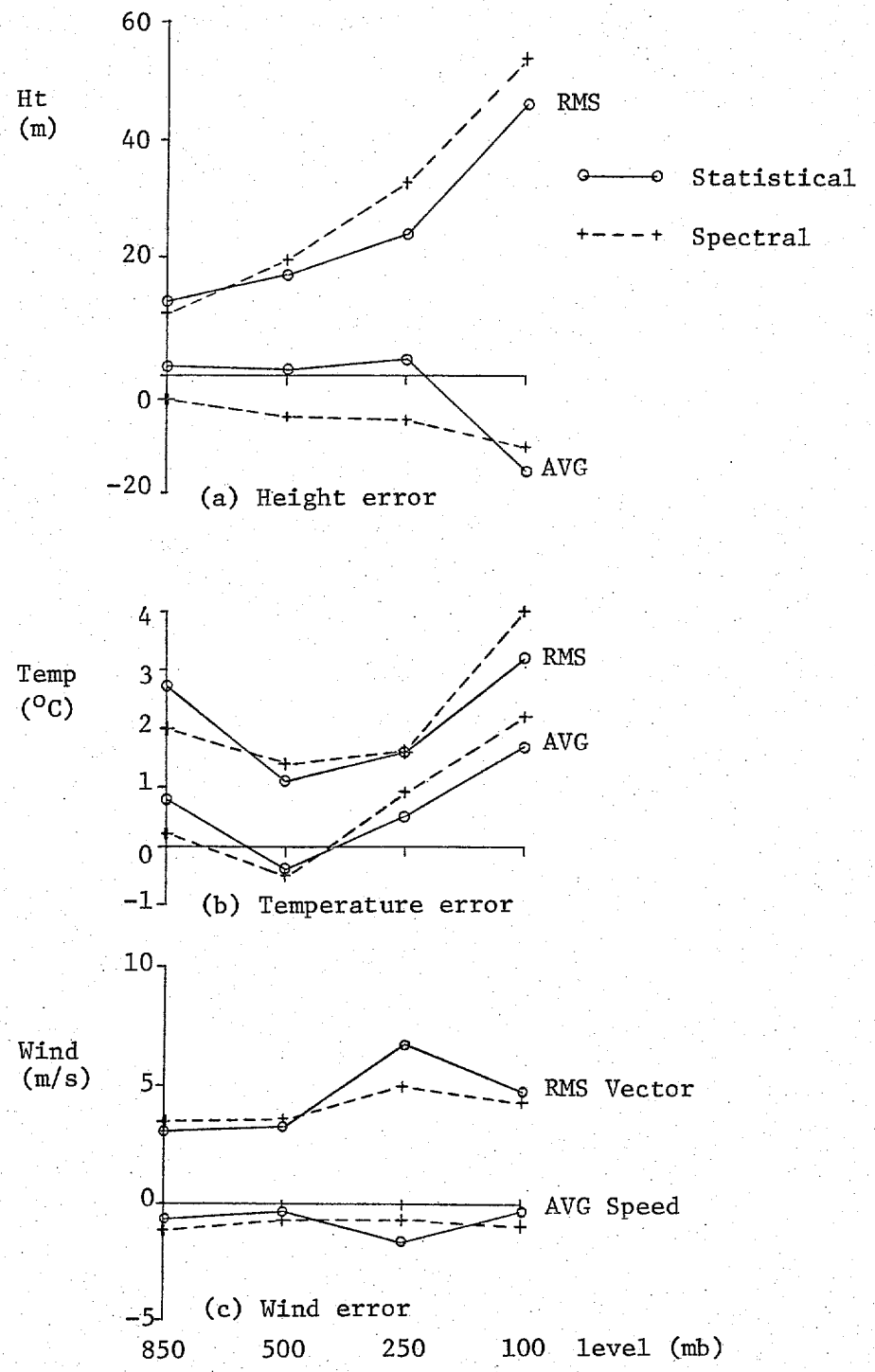

Figure 12. Average fit to 131 station rawinsonde network. Average of 12 cases.

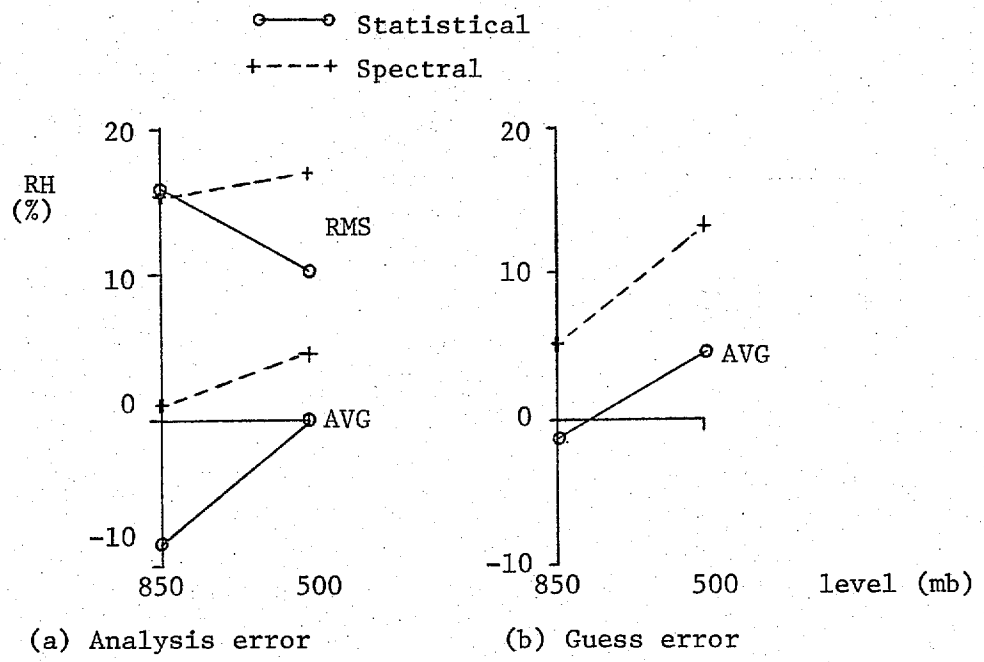

Figure 13. Analysis and guess relative humidity fit to 131 station rawinsonde network. Average of 12 cases.

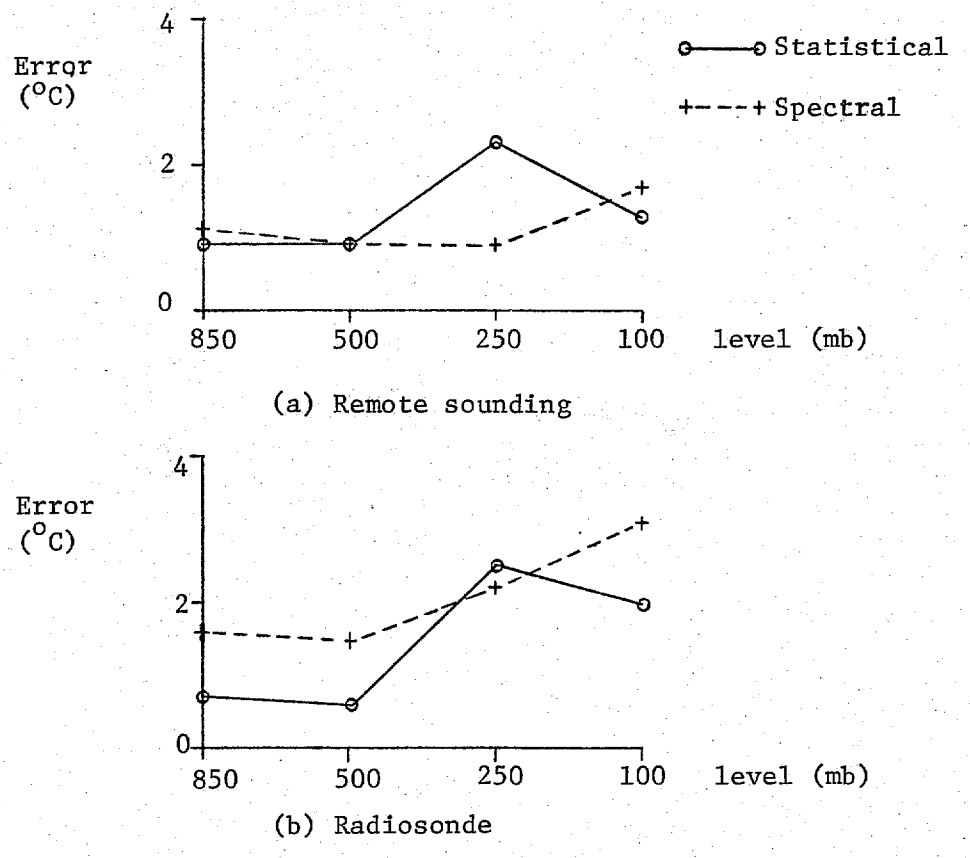

Figure 14. Root-mean-square fit of analysis to all thickness temperature data by type. Average of 12 cases.

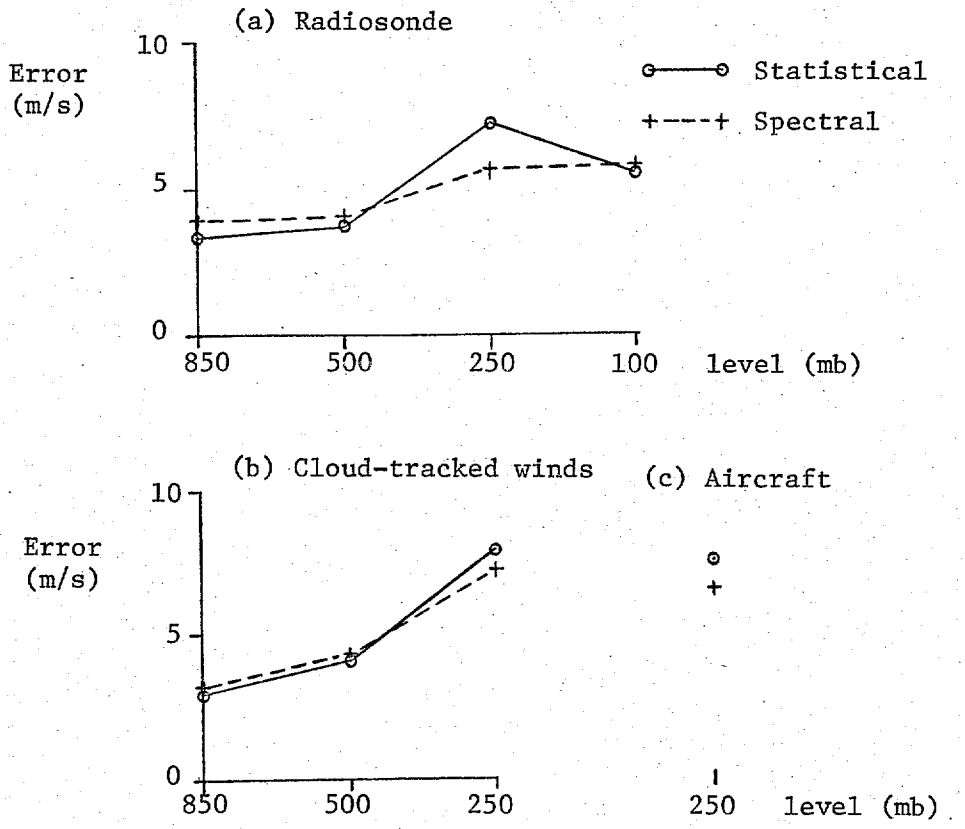

Figure 15. Root-mean-square analysis fit to all wind reports by data type. Average of 12 cases.

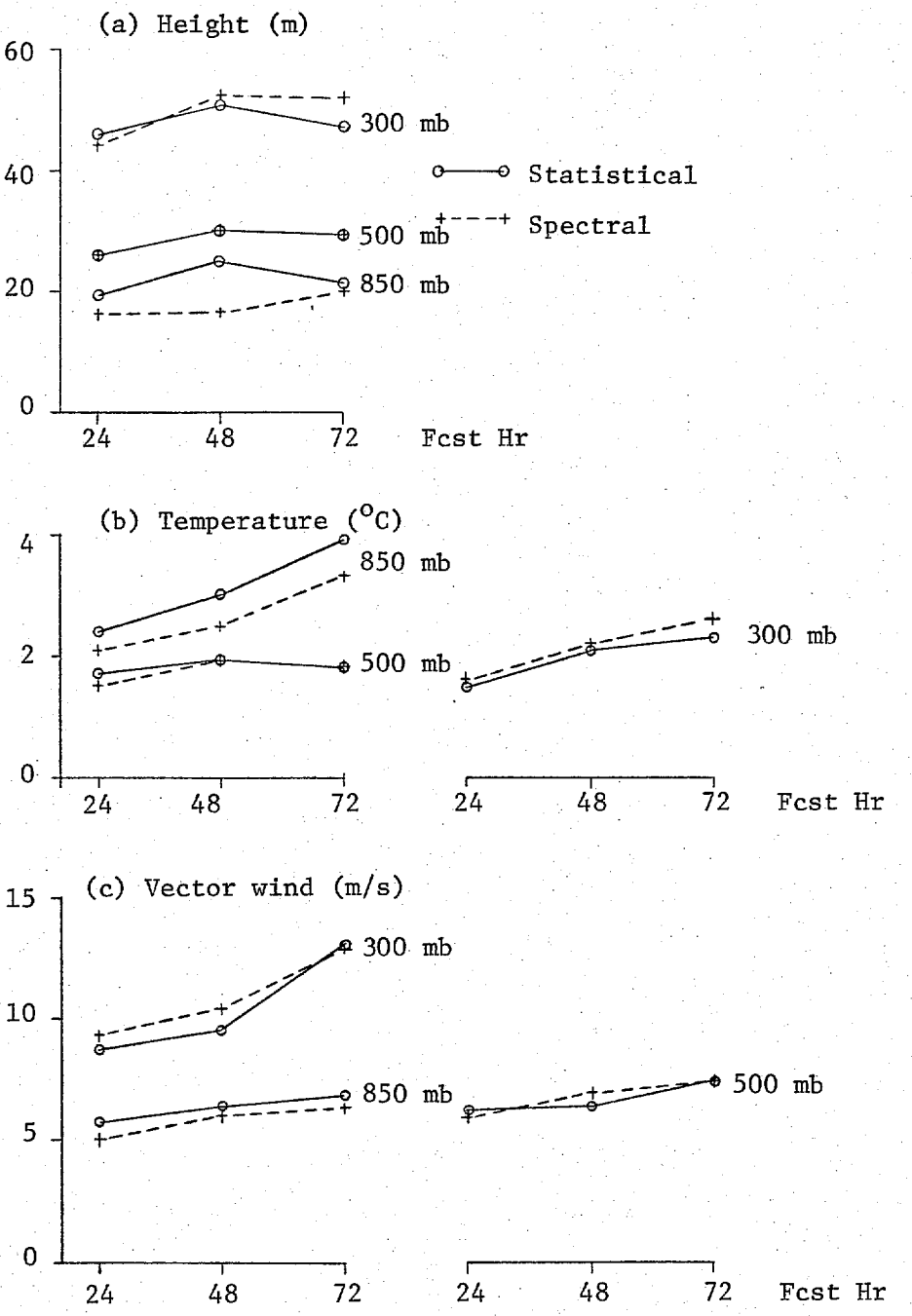

Figure 16. Three-layer forecast root-mean-square errors, verified against 131 station rawinsonde network. Initial time 0000 GMT 11 December 1977.

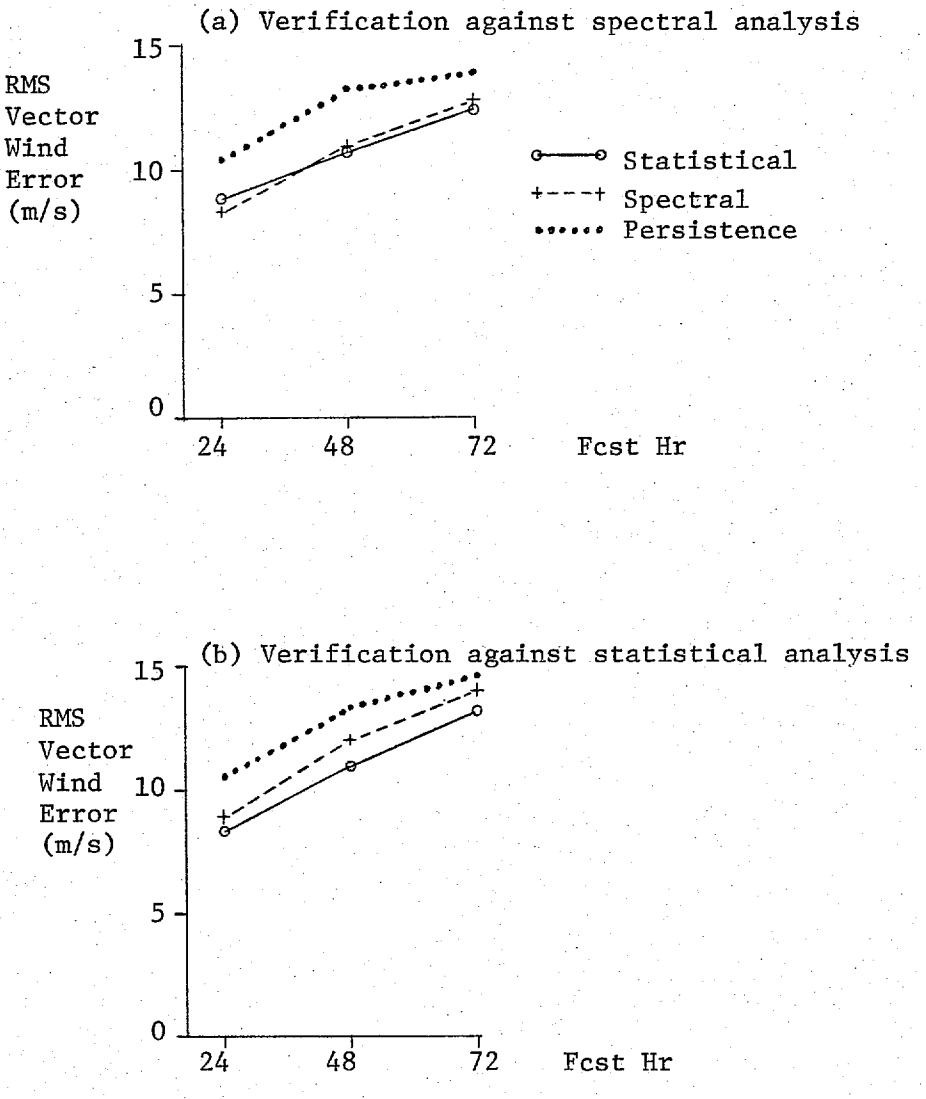

Figure 17. Three-layer 300-mb wind verifications against analyses. Initial time 0000 GMT 11 December 1977.